Title

Emerging superlubricity: A review of the state of the art and perspectives on future research

Journal

Applied Physics Reviews, 5(4)

ISSN

1931-9401

Authors

Baykara, MZ
Vazirisereshk, MR
Martini, A

Publication Date

2018-12-01

DOI

10.1063/1.5051445

Peer reviewed

Emerging superlubricity: A review of the state of the art and perspectives on future research

Mehmet Z. Baykara, Mohammad R. Vazirisereshk, and Ashlie Martini

Citation: Applied Physics Reviews **5**, 041102 (2018); doi: 10.1063/1.5051445
View online: https://doi.org/10.1063/1.5051445
View Table of Contents: http://aip.scitation.org/toc/are/5/4
Published by the American Institute of Physics

APPLIED PHYSICS REVIEWS—FOCUSED REVIEW

Emerging superlubricity: A review of the state of the art and perspectives on future research

Mehmet Z. Baykara,[a] Mohammad R. Vazirisereshk, and Ashlie Martini
Department of Mechanical Engineering, University of California Merced, Merced, California 95343, USA

(Received 8 August 2018; accepted 28 August 2018; published online 5 October 2018)

We present a review of superlubricity: the state of ultra-low friction between surfaces in relative motion. Various approaches to achieving this state are considered in a broad sense, including structural superlubricity, superlubricity via normal force control, and contact actuation, as well as thermolubricity, liquid superlubricity, and quantum lubricity. An overview of the physical fundamentals associated with each approach is presented, with particular emphasis on recent theoretical and experimental developments that constitute milestones in our scientific understanding. The review also includes a discussion of perspectives on future research in the context of existing challenges. It is projected that interest in superlubricity from the basic science and engineering communities will continue to accelerate in the near future, accompanied by a transition from fundamental studies to technologically relevant applications. https://doi.org/10.1063/1.5051445

TABLE OF CONTENTS

I. INTRODUCTION

Friction is undoubtedly one of the most common yet intriguing physical phenomena encountered in our daily lives. It would be impossible to play a stringed instrument or write with a pencil without the presence of friction and related effects. On the other hand, friction has a detrimental impact on global demand for energy and consequently environment and economy: About one fifth of the annual energy consumption on earth is used to overcome friction in a variety of systems and processes, from automobiles to manufacturing operations.[1] As such, methods devised to mitigate and control friction can have important implications for conservation of useful energy, increased lifetime of mechanical devices, and decreased environmental impact.

Despite the fact that there has been significant effort throughout history to reduce friction through improved lubricants, engineered surfaces, and optimized mechanical systems, the complex nature of the phenomenon has forced most of this work to be of an empirical nature. This is primarily due to the fact that friction is a complicated function of interface structure and chemistry, as well as environmental factors including temperature and humidity. Therefore, scientists have yet to develop a robust theoretical framework that can predict the frictional behavior of arbitrary sliding interfaces from first principles. Despite the difficulties associated with the formation of such a theoretical framework, in the past few decades, researchers have found novel ways to significantly reduce friction under certain conditions.

In the 1990s, Hirano[2,3] (and Sokoloff[4]) opened up a new avenue of thinking in friction research by carefully considering the details of the phenomenon on the atomic scale. In particular, they theoretically predicted that there exists a physical state where friction can nearly vanish if the sliding interface consists of surfaces that are atomically flat, rigid, structurally *incommensurate* (i.e., non-matching), molecularly clean, and weakly interacting. The mechanism underlying this state of ultra-low friction was that the lateral force experienced by almost every atom at the sliding interface would be systematically canceled out by the lateral force in the opposite direction associated with another atom, thereby resulting in negligible net friction force. This regime of ultra-low friction was called *superlubricity* by Hirano.[3] However, to avoid potentially confusing analogies with the

[a]Author to whom correspondence should be addressed: mehmet.baykara@ucmerced.edu

underlying physical principles of phenomena such as superconductivity and superfluidity, Müser later proposed the term *structural lubricity* (or *structural superlubricity*), highlighting the fact that the state of ultra-low friction in the case of incommensurate surfaces is mainly caused by a structural mismatch.[5] As will be discussed in this review, there are other mechanisms (i.e., other than structural) by which ultra-low friction can be achieved between surfaces at various length scales. As such, the term *superlubricity* is used here to describe any state of ultra-low friction (where, by widely accepted convention, the upper limit for the friction coefficient is taken to be 0.01[6]), whereas *structural superlubricity* specifically refers to the scenario of structurally incommensurate surfaces introduced above.

Immediately after the publication of Hirano's theory, there were several reports of experiments, suggesting superlubric sliding consistent with the theory of structural mismatch.[7–9] However, it took more than a decade to observe the first clear, quantitative experimental evidence of structural superlubricity: In 2004, Dienwiebel *et al*. used a modified atomic force microscope (AFM) in dry nitrogen to change the relative orientation of a graphite flake with respect to a highly oriented pyrolytic graphite (HOPG) substrate.[10] They observed that friction force strongly depended on the relative orientation angle of the flake and substrate, with a significant increase in friction at certain angles (corresponding to commensurate states) and vanishing values at all other orientations (corresponding to incommensurate states). A year later, Krylov *et al*. showed that temperature contributed to the superlubric behavior observed by Dienwiebel *et al*.[11] They proposed a new mechanism called *thermolubricity*, wherein friction is expected to vanish at high temperatures, low sliding velocities, and/or low corrugations of the interaction potential between the surfaces, based on the emergence of a thermal diffusion regime.[12] Taking a different approach, Socoliuc *et al*. showed in a series of AFM experiments that superlubricity can be achieved at the single asperity contact formed by an AFM tip on atomically flat substrates by (i) normal force control[13] or (ii) mechanical/electrostatic contact actuation.[14]

In general, there are two main challenges associated with the technological implementation of approaches used to achieve superlubricity at dry contacts: (i) the scaling-up of these approaches to conventional engineering length scales and (ii) the adaptation of related methods, which have been mostly limited to ultrahigh vacuum (UHV) or dry nitrogen atmosphere, to ambient conditions. However, these limitations have now been overcome in certain scenarios. In 2012, by performing experiments involving the detailed observation of *self-retraction* of graphite flakes on HOPG substrates, Liu *et al*. demonstrated that structurally superlubric sliding can indeed be achieved at the micro-scale and under ambient conditions, by implementing a novel approach to achieving flat, molecularly clean micro-scale interfaces.[15] Subsequently, a nano-island manipulation study by Cihan *et al*. provided quantitative confirmation of structural superlubricity under ambient conditions in an interface of dissimilar materials.[16] Additionally, the combined use of carbon-based materials such as diamond-like-carbon (DLC), nano-scale diamonds, and graphene under dry nitrogen has led to the observation of macroscale superlubricity, attributed by the authors to structural incommensurability effects.[17] As these selected examples illustrate, the possibility of using superlubricity to enable transformative improvements for mechanical systems, ranging from the potential prevention of wear over long periods of service to significant reductions in energy consumption, is now closer to reality than ever before.

The occurrence of superlubricity is not limited to solid interfaces, and it has indeed been demonstrated that the utilization of appropriate liquids (including ionic liquids) between surfaces in relative motion could lead to ultra-low friction sliding.[18–20] In particular, *liquid superlubricity* has been demonstrated in interfaces lubricated by low viscosity fluids that can shear easily, while at the same time providing sufficient load support. Also, recently, a new experimental technique utilizing a laser-cooled, one-dimensional (1-D) crystal of ions sliding over an optical lattice enabled the measurement of friction at the individual atom scale.[21] This approach could, in principle, lead to the experimental observation of *quantum lubricity*: a new theoretical concept in which quantum effects are expected to enable tunneling of ions through potential energy barriers, leading to an ultra-low friction regime.[22]

Considering the significant attention that the topic of superlubricity has received from the fundamental science and engineering communities,[6,23–29] we aim with this review article to cover developments in the field in a broad sense, with discussion of topics ranging from the well-known idea of structural superlubricity to more exotic proposals such as quantum lubricity. In particular, the fundamentals and milestone achievements associated with structural superlubricity are highlighted in Sec. II, followed by Sec. III, which is dedicated to superlubricity observed in AFM experiments via normal force control and contact actuation. Thermolubricity is described in Sec. IV, followed by a discussion of liquid superlubricity in Sec. V. Section VI includes a brief overview of 1-D friction experiments with laser-cooled ions and the possibility of quantum lubricity. Finally, Sec. VII concludes the review with a discussion of the current physical limits of the approaches used to achieve superlubricity, potential ways to overcome them, and future breakthroughs in applications that will be enabled once these limitations are overcome.

II. STRUCTURAL SUPERLUBRICITY

Among the various methods proposed for achieving ultra-low friction, structural superlubricity is considered to be one of the most promising. The scientific excitement surrounding structural superlubricity is, in part, due to the fact that the underlying physical principle is rather straightforward: Sliding at an interface formed by atomically flat, molecularly clean, weakly interacting, rigid surfaces with different lattice structures and/or incommensurate orientation should occur with vanishing friction. In other words, superlubric sliding at such interfaces is a direct result of their inherent geometry, which eliminates the need for exotic lubricants and/or elaborate *in-situ* methods to achieve a state of ultra-

low friction. While the mechanics underlying the expectation of structural superlubricity at such well-defined interfaces are explained in a number of detailed articles,[2,3,5,30] the main argument involves the fact that the lattice mismatch at structurally incommensurate interfaces causes the lateral force experienced by almost every atom in the interface to be negated by a corresponding atom, leading to a nearly vanishing net friction force. Conceptually, the effect of incommensurability involves the reduction of energy barriers against sliding. Structural superlubricity is fundamentally characterized by friction that depends sub-linearly on the contact area (for details on how the shape of the contact determines the scaling of friction with contact area, please see the discussion on nano-island manipulation below). The sub-linear dependence of friction force on the contact area constitutes a definitive sign of structural superlubricity and can be used instead of the more general definition of superlubricity that friction coefficients lower than 0.01.

The theoretical work by Hirano and Shinjo predicted the occurrence of structural superlubricity as early as 1990,[2] followed by significant hints of the phenomenon being captured in experiments performed using the surface force apparatus (SFA) at interfaces formed by mica[7,8] and molybdenum disulfide (MoS_2).[9] However, the first clear, quantitative experimental evidence of structural superlubricity came in the mid-2000s when Dienwiebel *et al.* showed using a custom atomic force microscope[31] operating under dry nitrogen that the friction force between a graphite flake and an HOPG substrate depended strongly on the relative, in-plane orientation of the flake relative to the substrate.[10,32] In particular, considerable friction was measured for relative orientations of the surfaces at multiples of about 60°, while the friction force measured at orientations even slightly different than these specific angles essentially vanished (Fig. 1). The results were explained within the framework of structural superlubricity: The specific orientations separated by 60° corresponded to *commensurate* structural configurations between the two surfaces (based on the six-fold symmetric, honeycomb structure of graphite), thus resulting in enhanced corrugations in the potential energy landscape and, as such, increased friction values. Other relative orientations resulted in an atomic-scale structural mismatch between the two surfaces, thus leading to a dramatic reduction of the potential energy corrugations and sliding with ultra-low friction. This trend was reproduced using atomistic simulations and simple 1-D models, which proved that the concept of canceling out of lateral forces on the atomic scale could explain the observed behavior.[33–37] It should be pointed out that later studies determined that the structurally superlubric state in the original set of experiments cannot be maintained over extended periods of time due to a torque-induced rearrangement of the interface to commensurate configurations.[38] Additionally, the stability of structural superlubricity for this particular material system has been theoretically studied as a function of sliding speed, sliding direction, temperature, and load.[39] Subsequently, experimental work was performed to investigate the robustness of structural superlubricity against the sliding distance: Feng *et al.* used scanning tunneling microscopy with high resolution at cryogenic temperatures to observe individual graphene nano-flakes on a graphene substrate transitioning between commensurate configurations and determined that sliding in the incommensurate state occurs across larger distances at lower temperatures.[40] Finally, a reversible switch from superlubric sliding to a high friction state was recorded for nanoscale graphene flakes sliding on HOPG with increasing normal force and attributed to out-of-plane deformation of the carbon atoms at the edge of the flake.[41]

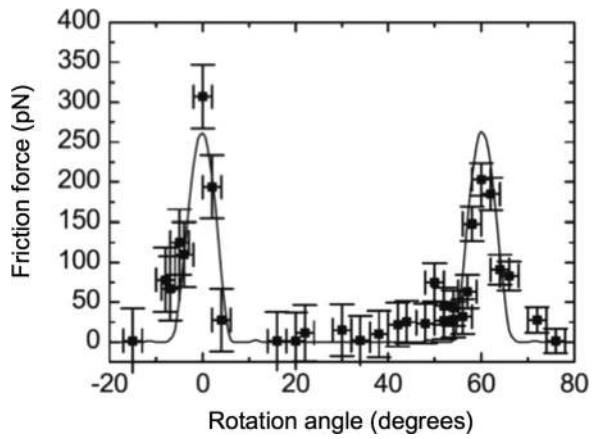

FIG. 1. Friction force experienced by a graphite flake on an HOPG substrate, as a function of the relative orientation designated by rotation angles around the axis normal to the substrate surface. Friction peaks around 0° and 60° correspond to commensurate configurations, while ultra-low friction values at other rotation angles correspond to structurally incommensurate orientations of the flake relative to the substrate, providing an elegant demonstration of the idea of structural superlubricity. Reprinted with permission from Dienwiebel *et al.*, Phys. Rev. Lett. **92**, 126101 (2004). Copyright 2004 American Physical Society.

For several years following Dienwiebel *et al.*'s pioneering experiments detailed above, surprisingly little experimental evidence of structural superlubricity was published. The associated difficulties were two-fold: (i) the fact that the observation of structural superlubricity requires an interface formed by atomically flat surfaces, which severely limits the available options for materials, and (ii) the requirement of molecular cleanliness at the interface,[37] which was, for a long time, thought to limit experiments to ultra-high vacuum (UHV) or at least dry nitrogen atmosphere. Experiments performed by Liu *et al.* in 2012 demonstrated an interesting approach to overcoming these two challenges.[15] Specifically, a micro-manipulator was used to laterally displace/shear graphite flakes from lithographically fabricated, micrometer-scale mesas on an HOPG substrate, whereby rapid lateral retraction of the flake to its original position on the mesa was observed [via scanning electron microscopy (SEM) under high vacuum and optical microscopy under ambient conditions] upon releasing the micro-manipulator from the flake's surface (Fig. 2). As the lateral forces associated with this *self-retraction motion*[42] due to a tendency to minimize free surface energy can be estimated with well-known parameters,[15] these forces set an upper limit for the friction encountered by the graphite flake as it slides back to its original position. The results (in comparison to those obtained by Dienwiebel *et al.*[10,32]) suggest that the friction forces are well within the superlubric regime, evidenced by measured

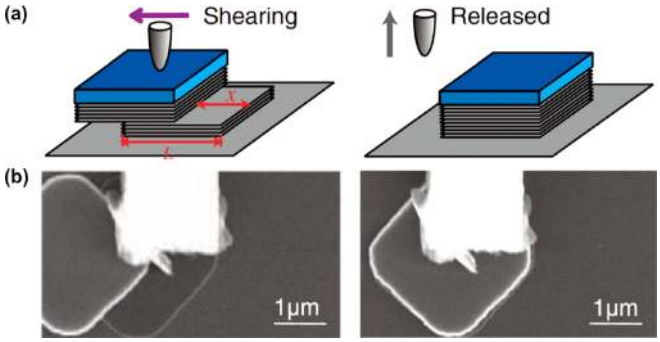

FIG. 2. **(a)** Schematic illustrations of a graphite mesa being sheared by the tip of a micro-manipulator and the subsequent self-retraction motion when the sheared flake is released. L is the side length of the mesa, while x is the distance traveled by the sheared flake. These parameters are used to calculate the force with which the sheared flake retracts back to its original position to minimize free surface energy. **(b)** SEM images acquired during the experiments, corresponding to the schematic illustrations. Reprinted with permission from Liu *et al*., Phys. Rev. Lett. **108**, 205503 (2012). Copyright 2012 American Physical Society.

shear stresses (0.02 to 0.04 MPa), which are about three orders of magnitude lower than the shear strength measured between commensurate basal planes of HOPG (0.1 GPa). Moreover, it is observed that the self-retraction motion is strongly suppressed (i.e., the flakes get *stuck*) when the sheared graphite flake is rotated against the mesa by specific angles at multiples of 60°, suggesting the *structural* nature of the observed superlubricity, in accordance with the six-fold symmetry of HOPG. A multi-scale model of this system that integrated density functional theory (DFT) calculations of the energetics driving flake retraction and molecular-dynamics simulations capturing the dynamic response of laterally offset surfaces demonstrated that nanoscale roughness can affect self-retraction motion.[43] Further studies on this peculiar experimental system with a high speed optical setup measured sliding speeds up to 25 m/s during self-retraction, demonstrating the robustness of superlubricity at high speeds.[44] In the same work, a certain degree of temperature dependence was identified in the observed superlubric sliding. The fact that structural superlubricity is preserved under ambient conditions has been attributed to a *nano-eraser* effect, whereby the edge of the retracting flake experiences out-of-plane deformation towards the underlying mesa during sliding, thus pushing contaminant molecules out of the way and preserving a molecularly clean interface.[27,45] Studies performed by Koren *et al*. on a similar material system were able to quantify friction forces between graphite flakes and mesas and confirmed their structurally superlubric nature.[46] Further experiments revealed that superlubricity can be observed for graphite flake junctions assembled under ambient conditions.[47] Moreover, in contrast to results obtained on nanoscale graphene flakes sliding on HOPG, the structural superlubricity of micrometer-scale graphite flakes does not appear to breakdown with an increase in normal force, up to pressures of about 1.70 MPa.[48] Although these experiments were performed on HOPG, model-based studies showed that self-retraction behavior can be expected for other 2D materials [including MoS_2 and hexagonal boron nitride (h-BN)[49]], followed by experiments quantitatively confirming superlubric behavior at homogenous junctions formed by MoS_2 sheets under high vacuum.[50] Additionally, following theoretical predictions,[51] heterogeneous junctions of graphite and h-BN have been very recently found to exhibit micro-scale superlubricity, under ambient conditions and at sustained normal loads up to 100 μm.[52] Overall, these studies demonstrated that a superlubric state attributable to structural effects can be observed under ambient conditions and at the micrometer scale (as opposed to the typically investigated nanometer scale). Furthermore, investigations performed on double-walled carbon nanotubes verified that structural superlubricity can be observed even at the macroscopic scale.[53] In particular, friction forces recorded during the telescopic extension of the inner tube of a double-walled carbon nanotube were found to be only in the range of a few nN (under ambient conditions and over pull-out lengths as long as a centimeter), which the authors attributed to the defect-free structure of the nanotubes and the geometric mismatch between the atomic structures of the inner and the outer tubes.

Noncontact atomic force microscopy (NC-AFM) enables the study of structural superlubricity with very high spatial resolution due to the atomic-scale imaging and force spectroscopy capabilities that it provides, combined with the fact that it can be used to laterally manipulate individual atoms and molecules on surfaces. As such, building on the methods established for molecular manipulation and related force measurements via NC-AFM,[54,55] Kawai *et al*. successfully measured structurally superlubric sliding of graphene nanoribbons on the crystalline Au (111) surface under UHV conditions and at cryogenic temperatures.[56] In particular, they showed (i) that the static friction force required to initiate sliding of graphene nanoribbons on Au (111) is below 100 pN for nanoribbons up to 22 nm in length (even lower than the static friction observed for, e.g., single atoms of Co on Cu (111)[54]) and (ii) that the static friction force per unit length drops with increasing nanoribbon length, essentially confirming that structurally superlubric sliding takes place. To study further the atomic-scale dynamics of graphene nanoribbons sliding on Au (111), the authors attached the tip of their AFM probe to the end of individual nanoribbons and then dragged them laterally on the Au (111) surface at fixed tip-sample distances [Figs. 3(a) and 3(b)]. The resonance frequency shifts experienced by the tuning fork in the NC-AFM system as a function of the lateral sliding distance reveal a stick-slip type motion of the nanoribbon as it slides on the Au (111) surface. The measured frequency shift is periodically modulated in steps of 0.28 nm [(Fig. 3(c)], a characteristic length arising from a particular configuration of the nanoribbon with respect to the underlying metal substrate. These experiments also indicate that local surface structure can affect superlubric sliding; specifically, the herringbone reconstruction of the Au (111) surface affects measured frequency shifts. Simulations complementing the experiments discussed here were performed in separate studies, suggesting that the short, 1D *edges* of the nanoribbons and not the 2D *bulk* are the main contributors to the observed stick-slip

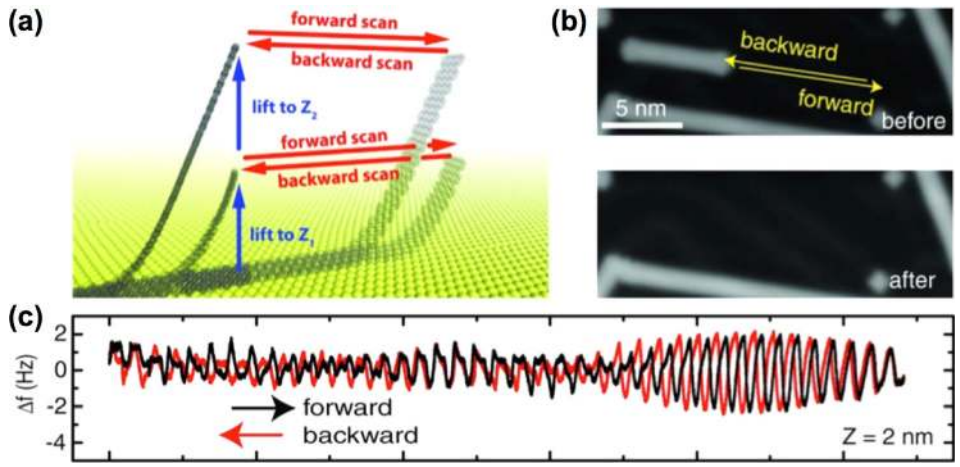

FIG. 3. **(a)** Illustration of an individual graphene nanoribbon being manipulated back and forth on an Au (111) substrate by the AFM tip attached at its end, at two different tip-sample distances of Z_1 and Z_2. **(b)** Scanning tunneling microscopy images of an area on the sample surface, before and after manipulation of a 6.28 nm long nanoribbon, demonstrating that the ribbon is lifted off the surface at the end of the process. **(c)** Resonance frequency shifts (Δf) of the AFM's tuning fork during the lateral manipulation of a nanoribbon (over a distance of ∼11 nm along the horizontal axis) at a tip-sample distance of 2 nm. The high frequency oscillations correspond to the stick-slip motion of the nanoribbon, while the slight modulation of the signal toward the end of the forward scan is due to the herringbone reconstruction of Au (111). Reprinted with permission from Kawai *et al.*, Science **351**, 957 (2016). Copyright 2016 AAAS.

friction;[57,58] a somewhat related idea was discussed earlier for physisorbed islands sliding on crystalline substrates.[59]

While NC-AFM has been useful for the study of structural superlubricity, its manipulation capabilities are essentially limited to individual atoms and molecules, and friction forces are not measured directly, but rather extracted from frequency shifts via analytical methods with certain assumptions. On the other hand, developing a comprehensive understanding of the main physical parameters that influence structurally superlubric sliding requires an experimental approach that allows the direct measurement of friction forces at sliding interfaces with varying size, shape, and chemistry and under varying experimental conditions, including but not limited to temperature and the presence/absence of vacuum. Within this context, the method of nanomanipulation via conventional, contact-mode AFM has been employed for more than a decade with great success to study frictional phenomena at interfaces formed by metallic nanoislands on atomically smooth substrates such as HOPG.[16,60–66] Specifically, Dietzel *et al.* demonstrated that both crystalline gold and amorphous antimony islands slide in a structurally superlubric fashion on HOPG under UHV, and that the friction forces scale sub-linearly with increasing contact area according to a power law.[63] The substantial variety in scaling power (0.33 ± 0.15) experienced by individual gold islands was attributed to differences in the shape of the islands, where an island with perfectly straight edges would experience either a scaling power of 0 (in cases when it is in an incommensurate registry with the substrate) or 0.5 (in cases when it is in a *pseudo-commensurate* registry with the substrate—which is expected to be a rare occurrence), and a perfectly round island would exhibit a scaling power of 0.25.[63,67] As the sharpness of island circumferences varies greatly in the experiments, so do the observed scaling powers, although all fall within the ultra-low friction regime imposed by structural superlubricity ($0 < \gamma < 0.5$). Following the 2013 paper by Dietzel *et al.*, Cihan *et al.* showed in 2016 that the occurrence of structural superlubricity at the gold−HOPG interface is not limited to the UHV environment but can also be observed under ambient conditions in a consistent fashion (Fig. 4).[16] This was the first quantitative confirmation of structural superlubricity under ambient conditions at an interface that did not involve carbon-based surfaces only[15,53] and as such paved the way toward robust, intrinsic lubrication schemes in nano- and micro-scale electro-mechanical systems with moving components. Based on *ab-initio* simulations employing DFT, the remarkable conservation of structural superlubricity under ambient conditions was attributed to steep energy barriers encountered by contaminant molecules trying to penetrate the gold−HOPG interface and the resulting preservation of molecular cleanliness.[16] The fact that gold does not oxidize under ambient conditions is critical in this process, as the crystalline, atomically flat and tight (separations on the order of 3 to 3.5 Å) interface between the islands and the HOPG substrate is kept intact over extended periods of time (at least several months), essentially acting as a microscopic *hermetic seal*. Further experiments by the same group have shown that structural superlubricity under ambient conditions is not limited to gold islands but can be extended to other noble metals such as platinum.[66] Moreover, these studies demonstrated the independence of the scaling factor relating friction to contact area from the chemical identity of the atoms forming the interface. While structural superlubricity at interfaces formed by different materials is now no longer restricted to UHV conditions, another limitation remains with respect to contact size and elasticity. Specifically, a number of theoretical studies involving elastic contacts have shown that structural superlubricity is expected to break down with increasing contact size, due to an Aubry-type transition[68] associated with the nucleation of local, structurally commensurate regions at the interface caused by atomic-scale elastic deformations.[69–71] Experimental confirmation of some of these predictions was recently published.[65,72,73]

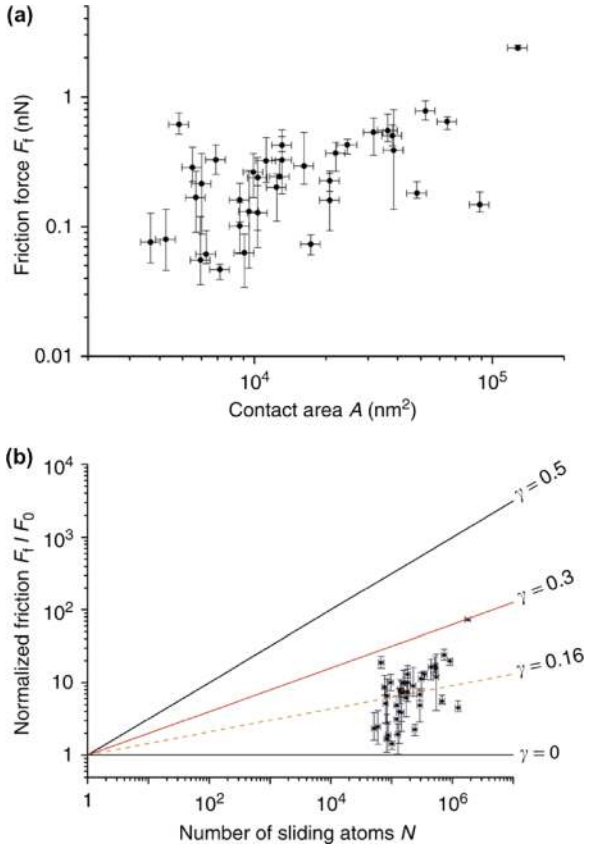

FIG. 4. **(a)** Friction forces recorded during nano-manipulation of gold islands on HOPG under ambient conditions, as a function of contact area. The friction is remarkably low, remaining below 1 nN for the great majority of manipulations, even for contact areas that approach the microscopic range. **(b)** Normalized friction forces plotted against number of gold atoms at the sliding interface. The values fall within the range of scaling powers (γ) relevant for structural superlubricity (0 to 0.5) and exhibit a mean scaling power of 0.16. The scatter is due to the variability in the circumferential shape of the islands. Reprinted with permission from Cihan *et al.*, Nat. Commun. **7**, 12055 (2016). Copyright 2016 Springer Nature.

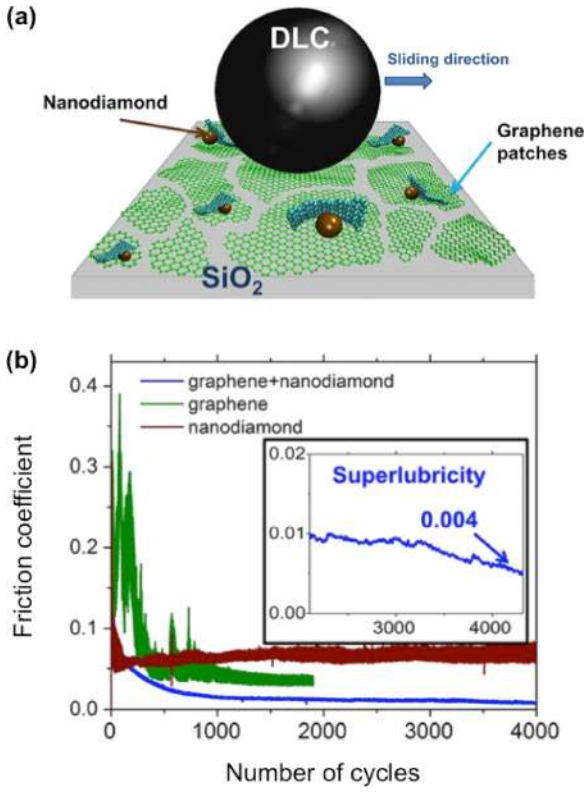

FIG. 5. **(a)** Illustration of the material system consisting of a DLC-coated slider on a SiO_2 substrate decorated with graphene patches and nanodiamonds. **(b)** Friction coefficient as a function of number of cycles in sliding experiments performed on substrates covered with nanodiamonds only (brown), graphene patches only (green), or both graphene patches and nanodiamonds (blue). The inset highlights the low friction coefficient associated with superlubric behavior observed for the latter case. Reprinted with permission from Berman *et al.*, Science **348**, 1118 (2015). Copyright 2015 AAAS.

The studies discussed above are certainly not the only observations of ultra-low friction in the literature that have been attributed to structural superlubricity. In a work published in 2015, researchers used a combination of carbon-based materials to achieve superlubricity at macroscopic length scales (with friction coefficients down to 0.004) and under dry nitrogen with a diamond-like-carbon (DLC) surface sliding against a SiO_2 substrate covered with patches of few-layer graphene and decorated with nanometer-sized diamond particles (i.e., nanodiamonds).[17] With help from electron microscopy and molecular dynamics simulations, the mechanism behind the observed superlubricity was found to be the formation of *nano-scrolls* (consisting of graphene patches wrapping around nanodiamonds), which act as miniature ball bearings between the sliding surfaces (Fig. 5). The researchers were subsequently able to achieve similar levels of superlubricity by using MoS_2 flakes instead of graphene, where sulfur atoms in MoS_2 facilitated the amorphization of nanodiamonds and the *in-situ* formation of *onion-like-carbon* particles during sliding, resulting in superlubric sliding.[74] In a recent study, it was shown that a composite film of amorphous carbon and onion-like-carbon particles also exhibited macroscale superlubricity.[75] Moreover, superlubric sliding was achieved between a graphene-coated silica (SiO_2) micro-sphere of 8 μm diameter and graphene as well as hexagonal boron nitride surfaces, at relatively high contact pressures of 1 GPa and up to relative humidity levels of 51%.[76] These experiments were complemented by further work in which it was shown that superlubricity can be obtained between an initially bare SiO_2 surface and graphite by tribo-induced transfer of graphene flakes onto the SiO_2.[77] It should be mentioned that, while the authors of the studies mentioned in this paragraph all attribute the superlubricity observed in their experiments to structural incommensurability between the contacting surfaces, direct, experimental confirmation of this hypothesis in accordance with established scaling laws is not possible, in contrast with, e.g., the nano-manipulation experiments discussed earlier.[16,63,66]

III. SUPERLUBRICITY VIA NORMAL FORCE CONTROL AND CONTACT ACTUATION

The majority of modern friction studies at the nanometer and atomic scales are conducted via AFM. The basic rationale behind the use of the AFM in friction studies is the idea that a complete understanding of friction—and ultimately, its control—at macroscopic contacts with multiple asperities

can be enabled by a fundamental understanding of friction at structurally well-defined, *single asperity* contacts, such as that represented by the tip of the AFM. Consequently, since its invention over three decades ago, AFM has been used extensively to study nanoscale friction on a variety of sample surfaces. Pioneering examples of such work include measurements of friction on lamellar solids such as HOPG[78] and mica,[79] ionic crystals,[80] metals,[81] and polymers.[82]

A theoretical understanding of the mechanics underlying AFM studies of friction is provided by the pioneering works of Prandtl[83] and Tomlinson[84] published about a century ago, which together form the so-called *Prandtl-Tomlinson* (PT) model. Their simple yet intuitive framework describes the motion of a point mass (corresponding to the tip apex in AFM experiments) over a periodic potential landscape (arising from the atomic-scale interactions of the tip apex with the sample surface) as it is dragged laterally over the sample surface by an elastic spring (representing the overall lateral stiffness of the system) attached to a support (corresponding to the base of the AFM cantilever) moving with constant speed. Assuming a sinusoidal potential arising from a crystalline surface for simplicity, the total energy of the system V (with contributions from the tip-sample interaction as well as the elastic potential energy stored in the spring) may be written as

$$V(x,t) = -\frac{E_0}{2}\cos\frac{2\pi x}{a} + \frac{k}{2}(vt - x)^2, \tag{1}$$

where E_0 is the corrugation (i.e., amplitude) of the tip-sample interaction, x is the lateral position of the tip, a is the period of the sinusoidal potential (corresponding to the lattice parameter of the crystalline surface), k is the *effective* spring constant (with contributions from the stiffness of the atomic-scale *contact* between the tip apex and the surface, as well as the lateral (i.e., torsional) stiffness of the body of the tip and the cantilever, all connected in series), v is the constant speed with which the support is moving laterally, and t is time. In the model, the tip apex moves between energy minima (i.e., $\frac{\partial V}{\partial x} = 0$) as the support pulls it over the surface, which implies

$$k(vt - x) = \frac{\pi E_0}{a}\sin\frac{2\pi x}{a}, \tag{2}$$

where $k(vt - x)$ represents the lateral force (F_L) detected by the AFM instrument. Under the assumption of a relatively soft spring (i.e., low k) and strong tip-sample interactions (i.e., high E_0), multiple solutions exist to Eq. (2), which correspond to the positions of potential energy minima x_i populated by the tip at different times during its motion over the surface. As the cantilever base moves laterally with increasing time with the tip in a particular potential minimum located at x_1, F_L grows continually until the potential energy stored in the spring is enough to overcome the energy barrier imposed by the tip-sample interaction, at which point the tip apex "jumps" to the next potential minimum at x_2, where it is "stuck" again. During the jump, the energy stored in the spring is dissipated, mainly through phononic channels.[85] These perpetual sequences of being stuck at and then jumping between potential minima—accompanied by energy dissipation—are referred to as "*stick-slip*" motion. Analysis of the mathematical model above shows that a relatively stiff spring (i.e., high k) and weak tip-sample interactions (i.e., low E_0) result in the disappearance of the *discrete* "stick-slip" type of motion in favor of a *continuous*, smooth sliding of the tip over the substrate, accompanied by vanishingly small average lateral forces and energy dissipation, i.e., *superlubricity*.[13,86] In particular, a parameter (η), describing the ratio of the tip-sample interaction strength to the elastic spring energy in the system, has been established to characterize the stick-slip vs. continuous character of the motion

$$\eta = \frac{2\pi^2 E_0}{ka^2}, \tag{3}$$

where $\eta > 1$ (obtained via strong tip-sample interactions and/or soft springs) is expected to result in stick-slip and $\eta < 1$ (obtained via weak tip-sample interactions and/or stiff springs) is expected to lead to superlubricity.

The obvious question that follows from the discussion above is whether the parameter η can be controlled reliably in an AFM experiment such that superlubric sliding can be deliberately *switched* on and off. To answer this question, the two components that determine η need to be considered: the effective spring constant k and the tip-sample interaction corrugation E_0. As indicated above, the effective spring constant k arises from a combination of the spring constants associated with (i) the atomic-scale contact region between the tip apex and the sample, (ii) the body of the tip, and (iii) the cantilever, connected in series. Consequently, the effective spring constant k is ultimately determined by the softest spring in the series, i.e., the contact stiffness (which is typically found to be on the order of a few N/m[13]). As the stiffness of the contact is determined by the structural arrangement and chemical identity of the individual atoms at the tip apex and the surface in the vicinity of the contact, it is not a parameter that can be easily accessed and altered in conventional AFM experiments. Therefore, studies have focused on manipulating the other parameter, E_0, to achieve superlubricity. Two approaches to manipulating E_0 are discussed in Subsections III A and III B: normal force control and contact actuation.

A. Superlubricity via normal force control

It is known that the interaction potential between two surfaces in contact can be altered by the normal force (F_N) acting between them.[87,88] In other words, pushing the two crystalline surfaces (or, for the sake of this discussion, the AFM probe and the crystalline surface over which it moves) together with a high normal force would increase the potential energy barriers that need to be surmounted for relative lateral motion. Realizing that the normal force is a parameter that can be freely changed in AFM experiments, Socoliuc *et al.* elegantly demonstrated in 2004 that the approach described above can be utilized to switch from the stick-slip to superlubric sliding regime.[13] In particular, they performed AFM experiments on ionic NaCl(001) surfaces under UHV conditions, where the lateral force traces were recorded

along the (100) direction in forward and backward orientations at varying normal forces (Fig. 6). The obtained results, supported by numerical solutions of the Prandtl-Tomlinson model introduced above, showed a clear transition from stick-slip to continuous/superlubric sliding with decreasing normal force, where continuous sliding was characterized by vanishing dissipation and average lateral force. Analysis of their results confirmed that the interaction corrugation (E_0) indeed increases with increasing normal force (more or less linearly) while the contact stiffness remains almost constant, with η values increasing with increasing normal force. Further experiments carried out on HOPG by Medyanik *et al*. under ambient conditions have shown that the phenomenon is not restricted to the UHV environment and that a regime of "*multiple slips*" (whereby the tip moves distances that are multiples of a when it *slips*) can be reached by appropriate choice of normal forces.[89]

The experiments introduced above are important from a fundamental point of view as they confirm an important aspect of the Prandtl-Tomlinson model: that superlubric sliding can be achieved by careful control of normal forces acting at a single asperity contact. On the other hand, the application of the results to a wide range of scenarios appears to be rather problematic as precise control of normal forces acting between surfaces in contact is simply not feasible in the majority of relevant mechanical systems. In contrast, the idea of structural superlubricity is rather robust against variations in normal force[48] and consequently has an advantage over the method discussed in this section in terms of applicability.

B. Superlubricity via contact actuation

Shortly after the demonstration of the use of precisely controlled, low values of normal forces to achieve superlubric sliding in AFM experiments,[13] a complementary approach based on the same theoretical framework was introduced.[14] In particular, Socoliuc *et al*. showed in their seminal paper from 2006 that the potential energy corrugation (E_0) experienced by the AFM tip apex as it is being slid over an atomically flat, crystalline surface can be periodically (specifically, in a sinusoidal fashion) modulated by electrostatic and/or mechanical actuation of the contact region in the direction perpendicular to the sample surface, leading to virtually vanishing friction (i.e., superlubricity) at well-defined actuation frequencies. In such a scenario, the effective energy landscape corrugation becomes[14]

$$E_{0,\mathrm{eff}}(t) = E_0(1 + \alpha\sin(2\pi f t)), \tag{4}$$

where f is the frequency with which the contact is actuated and α is a parameter between 0 and 1 with a value of 1 at resonance frequencies of the cantilever, when it is in contact with the sample surface (i.e., *contact resonance frequencies*). If the frequency of actuation is significantly higher than the frequency with which the AFM tip apex moves from one potential minimum to the next ($\frac{v}{a}$), the tip apex experiences the minimum effective energy corrugation ($E_0(1-\alpha)$) multiple times during its travel between adjacent potential minima. In this case, the key parameter that determines stick-slip

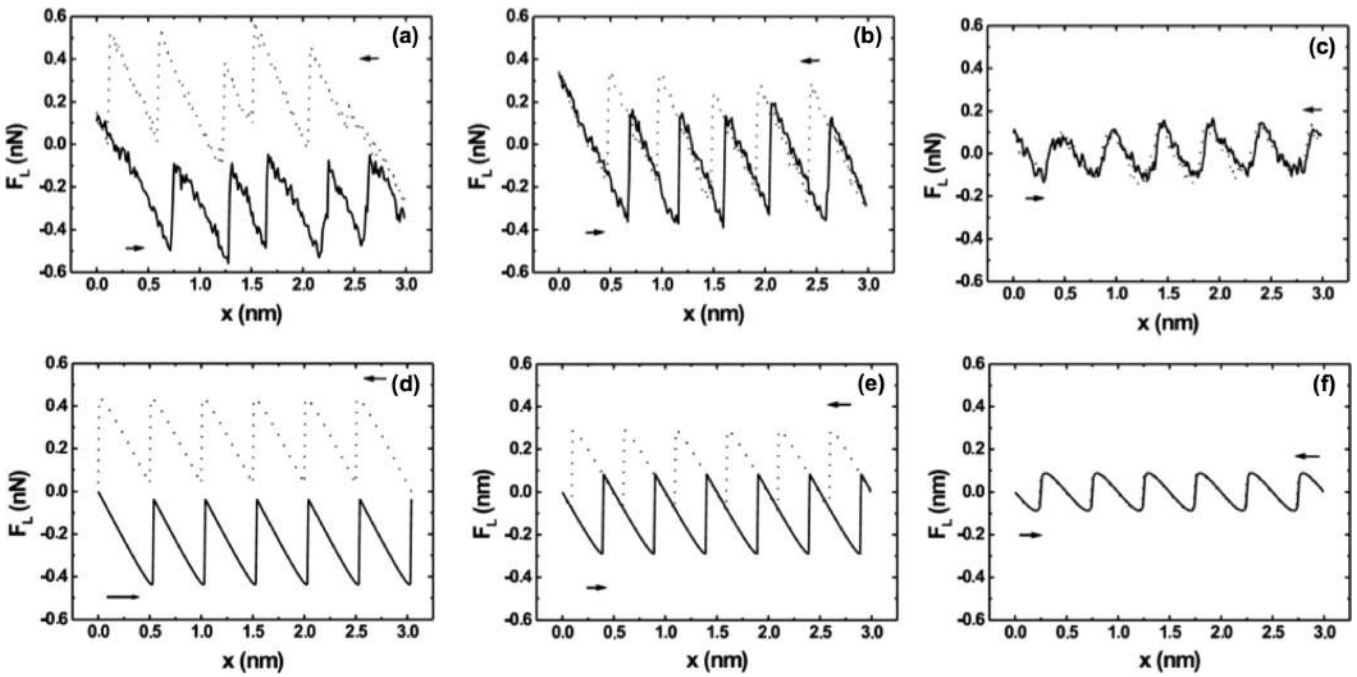

FIG. 6. **(a)–(c)** Traces of lateral force (solid line: forward scan, dashed line: backward scan) recorded on NaCl(001) via AFM at applied normal force values of (a) 4.7 nN, (b) 3.3 nN, and (c) −0.47 nN. The negative applied normal force in (c) indicates attraction, i.e., the tip is being pulled from the surface rather than pushed against it, essentially on the verge of separation (pull-off). With decreasing normal force, both the magnitude of the average lateral force and the amount of dissipation (quantified by the area enclosed by the hysteresis loop formed by forward and backward scan traces) decrease, practically vanishing in (c). **(d)–(f)** Numerically calculated lateral force traces using the Prandtl-Tomlinson model, with decreasing η values: (d) 5, (e) 3, and (f) 1. The numerical results closely follow the experimental trends, validating the basic ideas behind the Prandtl-Tomlinson model. Reprinted with permission from Socoliuc *et al*., Phys. Rev. Lett. **92**, 134301 (2004). Copyright 2004 American Physical Society.

vs. continuous (superlubric) motion (η) takes the following modified form:

$$\eta = \frac{2\pi^2 E_0(1-\alpha)}{ka^2}. \quad (5)$$

The implication of this expression is that the establishment of superlubric sliding ($\eta < 1$) becomes progressively easier with increasing α, which occurs when the contact established between the AFM tip and the sample surface is actuated at contact resonance frequencies.

The theoretical expectation described above was experimentally realized by Socoliuc *et al.*,[14] who showed a clear transition from stick-slip to continuous/superlubric sliding induced by electrostatic actuation of the tip-sample contact. Similar to their previous work involving normal force control,[13] they performed AFM experiments under UHV on ionic crystal surfaces (NaCl(001) and KBr(001)), where the application of an ac bias voltage between the cantilever and the conductive sample plates led to periodic electrostatic force/interaction energy modulations at the tip-sample contact. Their results demonstrated that vanishingly small average lateral forces and dissipation values can be recorded when the frequency of modulation matches the bending resonance frequencies (or half of them, due to capacitive effects) of the cantilever in contact with the sample surface (Fig. 7), in accordance with the theoretical framework described above.

After the pioneering work by Socoliuc *et al.*, further studies established the applicability of the method of contact actuation on multiple material systems and under different conditions. In particular, Gnecco *et al.* showed that superlubricity via contact actuation can be achieved under ambient conditions, and via mechanical (rather than electrostatic) methods induced by the application of an ac voltage to the piezo element used to excite the cantilever during dynamic AFM imaging.[90] This allowed the method to be extended from dielectric to conductive sample surfaces, e.g., HOPG.[90] The vanishing friction values obtained with contact actuation are naturally expected to lead to decreased wear and Lantz *et al.* were able to show that this is indeed the case in tip sliding experiments performed on a model polymer, with implications for extended probe lifetimes in mechanical data storage applications.[91] Further experiments performed on polymer surfaces complemented these findings and demonstrated the potential for controlled nano-patterning via deliberate contact actuation during AFM lithography experiments.[92] Moreover, theoretical analysis[93] and experiments[94] have shown that a state of vanishing friction and dissipation can also be achieved by lateral (i.e., *in-plane*) actuation of the tip-sample contact rather than perpendicular (i.e., *out-of-plane*) actuation. In the case of lateral actuation, the elastic energy stored in the spring coupling the tip apex to the AFM base is periodically modulated (rather than the tip-sample interaction corrugation) and superlubricity is achieved at room temperature when the lateral oscillation amplitude is roughly equal to one half of the lattice spacing a.[94]

IV. THERMOLUBRICITY

Several AFM-based experimental[95–99] and theoretical[11,12,100–102] studies have shown that temperature plays an important role in atomic-scale friction. The effect of temperature on friction was initially described by Prandtl in 1928,[83] where he predicted that friction should monotonically decrease as temperature increases due to thermal activation, via the contribution of thermal energy to overcome local energy barriers and enable slip. This behavior is captured by the Prandtl-Tomlinson model, introduced in Sec. III: At 0 K, in the absence of thermal activation, the point mass gets stuck in the minima of the interaction potential, until the energy stored in the effective spring is high enough to overcome the underlying energy barrier. At this point, the system is mechanically unstable, and the tip slips into the adjacent potential minimum. In this case, the friction force exhibits the typical saw-tooth pattern associated with stick-slip motion [Fig. 8(a)]. Thermal effects contribute to the reduction of friction in two different ways: (i) in a modest fashion, via thermal activation in the stick-slip regime and (ii) strongly, in the form of *thermolubricity* in the thermal drift regime.[11,12] To quantify these two regimes, Krylov *et al.* proposed a dimensionless parameter as follows:[11]

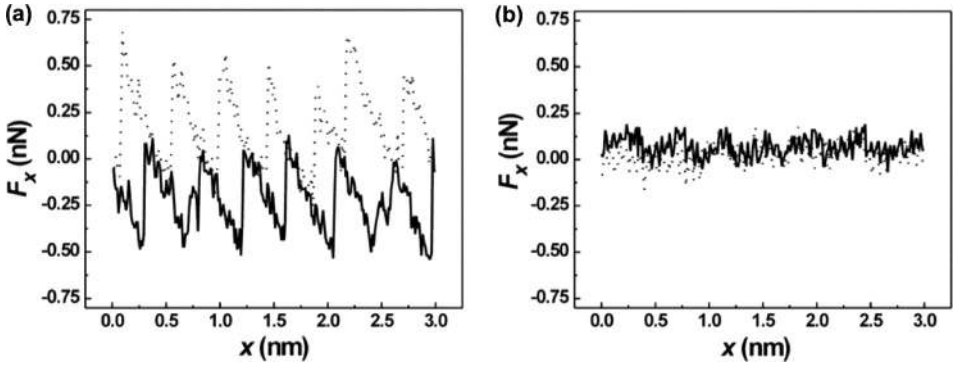

FIG. 7. **(a)** Traces of lateral force (solid line: forward scan, dashed line: backward scan) recorded on NaCl(001) via AFM at an applied normal force value of 2.73 nN, without contact actuation. **(b)** Traces of lateral force obtained during the same experiment session as in (a), with mechanical actuation of contact at a frequency of 56.7 Hz. Note the significantly reduced value of the average friction force, as well as vanishing dissipation illustrated by the fact that the forward and backward lateral force traces nearly overlap with each other. Reprinted with permission from Socoliuc *et al.*, Science **313**, 207 (2006). Copyright 2006 AAAS.

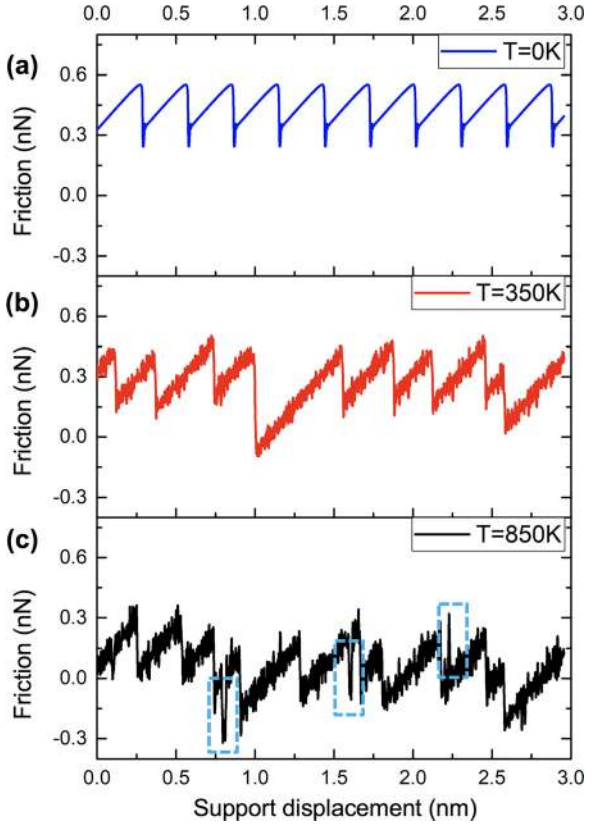

FIG. 8. Representative friction traces calculated using the Prandtl-Tomlinson model at three different temperatures of **(a)** 0 K, **(b)** 200 K, and **(c)** 800 K. With increasing temperature, friction decreases, and back and forth jumps of the tip are observed; some examples are highlighted by the dashed blue rectangles in (c).

$$\beta = \frac{v}{af_0}\exp\left(\frac{E_0}{k_B T}\right), \tag{6}$$

where v is the support's speed, E_0 and a are the amplitude and period of the idealized (i.e., sinusoidal) tip-sample interaction potential, respectively, k_B is the Boltzmann constant, T is the temperature, and f_0 is the *attempt rate* (i.e., frequency) for thermally activated jumps, which is typically considered to correspond to the frequency of tip apex vibrations.[88] The attempt frequency is assumed to be constant in most studies; however, it was also suggested that this parameter could vary with temperature[97] and with the characteristics of the potential energy landscape.[102]

Within the framework of the model outlined above, low temperatures and/or high velocities ($\beta \gg 1$) result in the occurrence of the conventional stick-slip regime, where the backward energy barrier can be assumed to be much higher than the forward energy barrier, and therefore backward slips can be neglected.[12] In this case, thermal effects facilitate the tip's ability to slip to the adjacent surface potential minimum in the forward direction, prior to reaching the mechanical instability point. Consequently, these thermally activated jumps cause the maximum lateral force of the spring in the Prandtl-Tomlinson model to decrease, and as a result, friction is lower [Fig. 8(b)]. As temperature increases, more thermal energy becomes available, which increases the probability of such thermally activated jumps and further decreases friction. It should be also mentioned that, in the stick-slip regime, friction has been found to depend logarithmically on sliding velocity, based on the idea that at higher speeds there is less time for thermally activated jumps.[99,103,104]

When the temperature is sufficiently high and the velocity is low ($\beta \ll 1$), the system can be considered to be continuously in thermal equilibrium, and frictional behavior evolves from stick-slip to a stochastic thermal drift regime. Thermal excitations are now much stronger and the probability of having backward slips cannot be neglected.[12] Due to the low velocity of the support in this case, the tip exhibits several thermally activated back and forth jumps as the cantilever base moves from one lattice position to the next one [Fig. 8(c)]. Instead of simply facilitating slip events in the forward direction when the system is on the verge of mechanical stability, thermal effects now allow the tip to overcome potential energy barriers altogether and the tip apex *diffuses* over the potential energy landscape (both in the forward and backward directions), while the support moves with constant velocity in the forward direction. This phenomenon, which is characterized by vanishing friction and the disappearance of stick-slip behavior in favor of stochastic fluctuations in friction force, is termed *thermolubricity*. In this regime, the dependence of average friction on temperature and velocity has been described as[12]

$$F_f \propto v\left(\frac{k}{f_0}\right)\frac{E_0}{k_B T}\exp\left(\frac{E_0}{k_B T}\right), \tag{7}$$

where friction now depends linearly on sliding speed (as opposed to the logarithmic velocity dependence expected for the stick-slip regime), and even minute changes in temperature and potential corrugation can result in significant modulation of friction, thanks to an exponential dependence on these parameters.

The concept of thermolubricity discussed above has been further explored by simulation studies. For example, Steiner *et al.* used a two-dimensional (2-D) Prandtl-Tomlinson model to analyze the effect of temperature on friction between an atomically sharp tip and substrates of NaCl and HOPG.[105] They showed that, above a critical temperature (which depends on the interaction energy corrugation), the system transitions into the thermolubricity regime, where the average friction force becomes vanishingly small. Further work by Iizuka *et al.* numerically analyzed the role of temperature in superlubric sliding achieved by contact actuation (see Sec. III) by performing simulations based on the Prandtl-Tomlinson model.[106] Their results revealed that the critical modulation amplitude for reaching superlubricity at room temperature is considerably smaller than the critical modulation amplitude at zero temperature, highlighting the role that thermal effects play in superlubricity achieved via contact actuation. Finally, accelerated atomistic simulations coupled with numerical solutions to a kinetic model predicted the complex friction-temperature-sliding speed landscape over a temperature range of several hundred degrees, and speeds across six orders of magnitude (Fig. 9).[107]

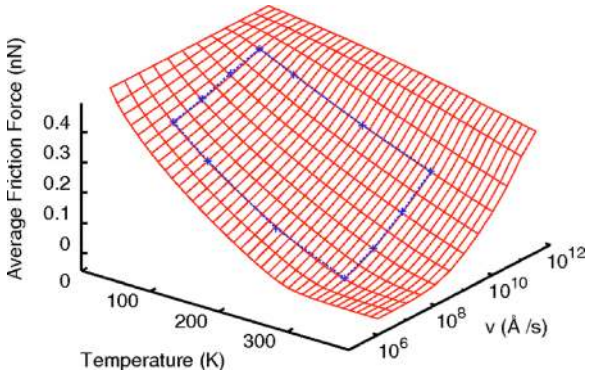

FIG. 9. Average friction force as a function of temperature and scanning velocity calculated using a kinetic model (red surface) and atomistic parallel replica dynamics simulations (blue symbols and dotted line). Reprinted with permission from Perez *et al.*, Phys. Rev. B **81**, 245415 (2010). Copyright 2010 American Physical Society.

As suggested by Eq. (6), thermolubricity can, in principle, be achieved by lowering the velocity or increasing the temperature, as well as by reducing the corrugation of the tip-sample interaction potential. This idea was tested by re-analyzing[12] the pioneering experimental work by Dienwiebel *et al.*[10] (discussed in Sec. II). Figure 10(a) shows three friction traces for fully commensurate, partially commensurate, and fully incommensurate configurations of the flake with respect to the substrate, corresponding to $\eta = 5.25$, $\eta = 3.33$, and $\eta = 2.47$, respectively (note that all η values are above the superlubricity limit of 1). As η decreases, both the magnitude of the friction force and the character of the friction trace change. In particular, while the friction force decreases, the regular stick-slip trend observed in the fully commensurate configuration changes first to irregular stick-slip in partially commensurate contact, and then to a stochastic drift pattern in the fully incommensurate case. This qualitative observation suggests that, for a small contact close to the superlubricity limit, thermal effects can be so strong that one can observe ultra-low friction even when $\eta > 1$, due to the effect of thermolubricity.[12] This observation provided an improved explanation for the results previously attributed only to structural superlubricity, by shedding light on the role of temperature in the observed superlubric behavior. Moreover, the experimental data have been fitted by the thermolubricity model discussed above [see Eq. (7)] for specific attempt frequencies (the only free parameter in the model), and the occurrence of thermolubricity was confirmed by noting that experimentally recorded friction values are consistently lower than the predictions of the conventional (i.e., temperature-independent) Prandtl-Tomlinson model, where thermal effects are not taken into consideration [Fig. 10(b)].[12]

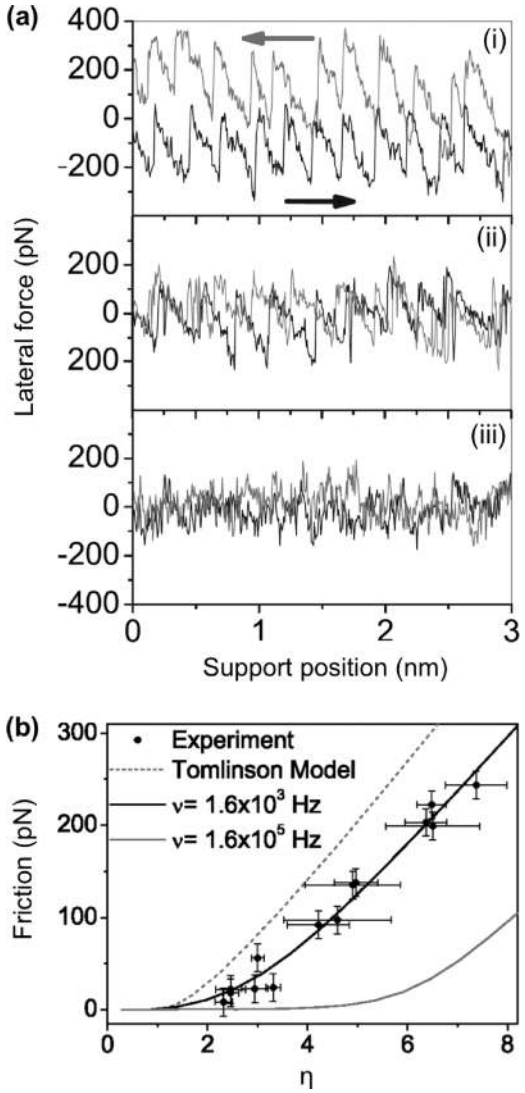

FIG. 10. **(a)** Forward (dark) and backward (light) experimental friction traces obtained at the interface formed by a graphite flake and HOPG substrate, for fully commensurate (i), partially commensurate (ii) and fully incommensurate (iii) configurations, with calculated η values of 5.25, 3.33, and 2.47, respectively. The gradual evolution from stick-slip behavior to stochastic fluctuations in the friction trace and the accompanying decrease in average friction are observed with decreasing η values. **(b)** Experimental friction data vs. η, fitted to the thermolubricity model (solid lines) with two different attempt frequencies (given here using the symbol ν instead of f_0). The dashed line represents the temperature-independent Prandtl-Tomlinson model, which is devoid of thermal effects and thus systematically overestimates friction values. Reprinted with permission from Jinesh *et al.*, Phys. Rev. B **78**, 155440 (2008). Copyright 2008 American Physical Society.

V. LIQUID SUPERLUBRICITY

So far in this review, superlubricity has been considered only at dry contacts. However, some interfaces are necessarily lubricated by liquids, where the liquids not only separate sliding surfaces but also remove heat and/or carry contaminants away from the interface. Generally, friction in liquid-lubricated contacts is determined by the lubrication regime, which depends on several different parameters, including the viscosity of the liquid, sliding speed, contact pressure, and surface roughness. Lubrication regimes are typically illustrated by the so-called Stribeck curve, which describes the transition from boundary lubrication (contact between dry surfaces or surfaces with adsorbed chemicals) to mixed lubrication (load supported by a combination of liquid and solid contacts within the interface) to full film lubrication (load entirely supported by the lubricant). As speed or viscosity increases, or pressure decreases, the fluid film thickness increases until it is thicker than the composite roughness of the surfaces and full film lubrication is achieved. Friction is typically lowest at the onset of full film lubrication, where the fluid is thick enough to

completely separate the surfaces, but thin enough to provide low viscous friction.

For more viscous fluids, like oils, a typical full film friction coefficient might be on the order of 0.1; for less viscous fluids, like water, friction will be even lower. Therefore, interfaces lubricated by low viscosity fluids are already quite close to the traditionally accepted limit of superlubricity (friction coefficients lower than 0.01) under certain conditions. However, studies have demonstrated that such interfaces can exhibit a lower-than-expected friction coefficient by creating conditions that involve smooth surfaces, a thin liquid film (for low viscous friction), and a high load carrying capacity. The challenge is that the latter two are usually mutually exclusive, i.e., films that can support a large normal force usually have high resistance to shear, and vice versa. Thus, studies on liquid superlubricity are focused on finding ways to overcome this challenge, typically by using water or another low viscosity liquid as the lubricant.

Early work on liquid superlubricity reported ultra-low friction for water-lubricated, self-mated Si_3N_4.[108] Based on the observation that surfaces were very smooth after testing, the authors hypothesized that tribo-chemical reactions caused wear to occur molecule-by-molecule, yielding very smooth surfaces such that full film lubrication could exist for thin water films with low viscous friction. Although this is likely a simplified view of the complex mechanisms that enabled superlubricity in the study, it clearly shows that smooth surfaces are required to achieve very low friction. In all studies described here, very smooth surfaces were either formed during the test or explicitly part of the experimental design.

In addition to smoothing surfaces, chemical reactions between the lubricant and solids in a sliding interface can result in the formation of a so-called tribofilm. Tribofilms form via tribo-chemical reactions in which shear accelerates chemical reactions, sometimes by changing the reaction pathway.[109,110] These films typically have very low shear resistance and can be removed and replenished in the interface during sliding. It is difficult to directly interrogate tribofilms because they form and function inside of a sliding interface, so hypotheses about tribofilms are typically based on observations of very low friction (measured using ball/pin/cylinder-on-disk instruments at pressures of hundreds of MPa) and post-test surface analyses (e.g., SEM). Several studies with water-lubricated, self-mated Si_3N_4 reported superlubricity[111–114] and suggested that friction was reduced (beyond what is expected from surface smoothing alone) by a decrease in the contact pressure coupled with tribo-chemical reactions that resulted in the formation of a tribofilm consisting of soft colloidal silica[111] or silica "gel."[114] This mechanism was further explored for Si_3N_4 sliding on glass with various low viscosity lubricants, including phosphoric acid,[115–117] glycerol/acid mixtures,[19] and polyhydroxy alcohol/acid mixtures.[118] The proposed mechanism for the superlubricity was the formation of a hydrogen-bond network that enabled a thin water layer at the interface, such that sliding occurred within the water with very low friction. This hypothesis was supported by evidence showing the dependence of friction on the PH of the liquid.[19,117] Beyond Si_3N_4, ultra-low friction was also observed for self-mated tetrahedral amorphous carbon (ta-C) with glycerol, and complementary simulations suggested the decomposition of the glycerol in the interface and the formation of a hydrogen bond network tribofilm.[119] The same authors were able to measure superlubricity with self-mated steel as well, with a mixture of glycerol and inositol, and proposed a similar mechanism as that for ta-C. Finally, superlubricity was observed for steel sliding on a nickel-titanium alloy (60NiTi), with castor oil lubrication.[120,121] The proposed mechanism of superlubricity was a tribofilm that can support additional load due to repulsive electrostatic forces acting between intercalated metal oxy-hydroxide lamellar compounds.[121] However, a later study with the same materials was not able to reproduce the ultra-low friction.[122]

Several studies described above proposed a mechanism in which the tribofilm provides extra load support through a hydrogen bond network that enables a very thin layer of water to accommodate shear. However, in these studies, it was difficult to isolate the effect of this load support mechanism from the effects of surface smoothening and decreased pressure. To address this, studies have been performed using surface forces apparatus/balance (SFA/SFB) setups. In these experiments, forces are measured on aqueous solutions confined between atomically smooth mica surfaces and subject to relatively low pressures, typically less than 1 MPa. The conditions are such that there is no wear and the pressure is constant, and measurements can be performed down to just a monolayer of water molecules. This approach isolates the load-carrying capacity of the liquid from other factors. Such studies have shown that superlubricity can be achieved through a *hydration layer*.[123,124] Hydration layers support large pressures without being squeezed out and also relax very rapidly so they can exhibit a fluid response to shear, see Fig. 11. This mechanism was reproduced by molecular dynamics simulations as well.[125] It is notable that this mechanism is possible with aqueous solutions because confinement suppresses their tendency to solidify, in contrast to most non-associating liquids, including lubricating oils. The topic of hydration layers is reviewed comprehensively in Ref. 18. A related mechanism has been observed in ionic liquids. Ionic liquids are molten salts that are typically composed of larger organic cations and smaller organic or inorganic anions.[126] SFA/SFB and AFM studies have shown that superlubricity can be achieved with ionic liquids confined between charged, atomically flat (usually mica or graphite) surfaces.[20,127,128] It is proposed that the irregular shapes of the ions inhibit solidification and locking, which leads to a low shear stress, while strong Coulombic interactions between the ions and the charged confining surfaces provide load support.[127] Interestingly, friction with ionic liquids has been shown to be tunable with electric potential (Fig. 12)[20] and ion structure.[129] Most of these studies have been performed with atomically flat surfaces and at low pressures, but ionic liquids have also been considered for larger scale engineering applications as both base fluids and additives[126] and studies have shown that they can yield friction in mixed lubrication that approaches the superlubricity regime.[130]

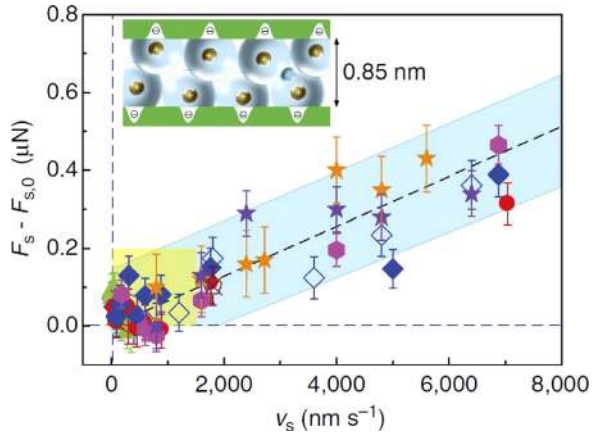

FIG. 11. Variation of shear forces with sliding velocity from SFA/SFB experiments illustrating the ultra-low friction that can be achieved with a hydration layer. The inset illustrates the structured hydration layer that is formed between the solid surfaces (which can both support a load and shear easily), leading to liquid superlubricity. Reprinted with permission from Ma *et al.*, Nat. Commun. **6**, 6060 (2015). Copyright 2015 Springer Nature.

A third mechanism of superlubricity is observed with very soft materials, specifically polymer brushes[131] and hydrogels. In general, the concept is that polymers can be both solid-like, to provide load support, and liquid-like, to shear easily. In the case of polymer brushes, chain molecules are grafted onto two contacting surfaces and friction is measured at pressures typically below 10 MPa. The chain structures are ordered and can swell with water such that they can support normal forces, but the interface (or overlap) between the ends of the polymers on the two surfaces is fluid-like and provides superlubricity.[132–138] The performance of these brushes has been optimized by tuning the length of the polymers (longer chains yield lower friction)[134] and adding polymers to the buffer solution which provides self-healing capability at higher loads.[135] For charged brushes, even better performance has been observed, due to the formation of a hydration layer between the two polymer surfaces.[132,136,139] At low or moderate compressions, the brushes interpenetrate and the mechanism of superlubricity is configurational

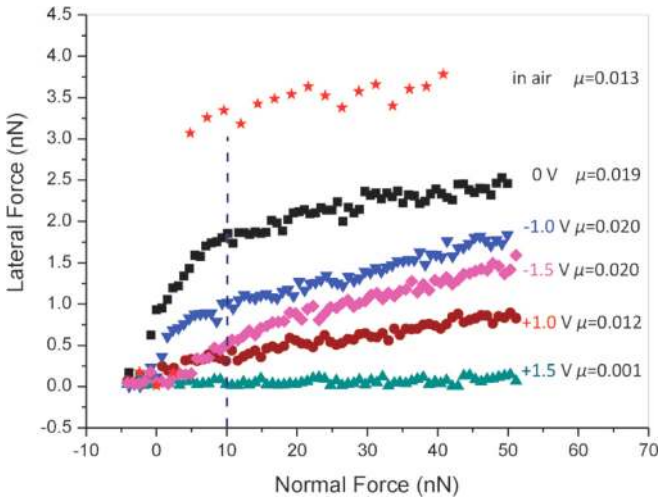

FIG. 12. Superlubricity is achieved in ionic liquid-lubricated interfaces by tuning the electric potential. Reprinted with permission from Li *et al.*, Chem. Commun. **50**, 4368 (2014). Copyright 2014 Royal Society of Chemistry.

entropy, as observed for neutral chains. However, at higher pressures, it is proposed that osmotic pressure of the trapped counter-ions provides additional load support, while a hydration layer provides low friction.[18] Although many polymer brush experiments are performed with small scale contacts (SFA/SFB or AFM), the efficacy of this lubrication method has been demonstrated for larger contacts as well.[133,138] Similar mechanisms are proposed for hydrogels, insoluble polymers that expand in water. Pin-on-disk measurements of self-mated hydrogels showed that superlubricity was achievable and the behavior was attributed to the ability of the bulk material to support the normal force, while the interface exhibits low shear resistance due polymer fluctuations on the surfaces.[140–142] However, the mechanisms of superlubricity in hydrogels are likely to differ somewhat from those of polymer brushes because polymer brushes are grafted onto rigid surfaces while hydrogels are self-standing and soft, resulting in much larger contact areas and much lower pressures.[140]

In summary, liquid superlubricity is achieved with systems having the following characteristics: (i) very smooth surfaces, (ii) low viscosity liquids, (iii) sufficient load support, and (iv) low shear resistance. Smooth surfaces can be achieved by surface wear during sliding, the formation of a smooth tribofilm during sliding, or design of experiments with inherently smooth surfaces (as in SFA/SFB) or soft materials (polymer brushes or hydrogels). Additionally, most studies are performed with very low viscosity fluids, most commonly aqueous solutions. The last two conditions (i.e. sufficient load support and low shear resistance) are the main challenges in liquid superlubricity and are the focus of most studies. An interface that is strong in the normal direction and weak in the shear direction has been achieved: (a) by forming tribofilms with low shear stress that can be replenished during sliding, (b) through a thin, ordered layer where the structure of the layer provides load support while still being fluid in the shear direction, and (c) with polymer materials that can be solid-like in the bulk or ordered regions but are fluctuating and fluid-like at the interface. It is likely that many observations of superlubricity at the macroscale combine more than one of these mechanisms.

VI. FRICTION WITH COLD IONS AND QUANTUM LUBRICITY

Sections III and IV discussed superlubric behavior in terms of the Prandtl-Tomlinson (PT) model, which approximates an atomic-scale friction experiment as a point mass being dragged over a 1-D sinusoidal potential energy profile. This model has been extended to incorporate multiple point masses in the contact region within the framework of the Frenkel-Kontorova (FK)[143,144] and Frenkel-Kontorova-Tomlinson (FKT)[36] models. The difference between these models is illustrated in Fig. 13. The FK and FKT models enable predictions of friction as a function of the lattice spacing, size, and stiffness of a moving array of point masses.[145]

Analytical and numerical studies predicted that FK/FKT behavior could be observed experimentally with cooled ion chains in optical lattices (i.e., standing waves) for over a

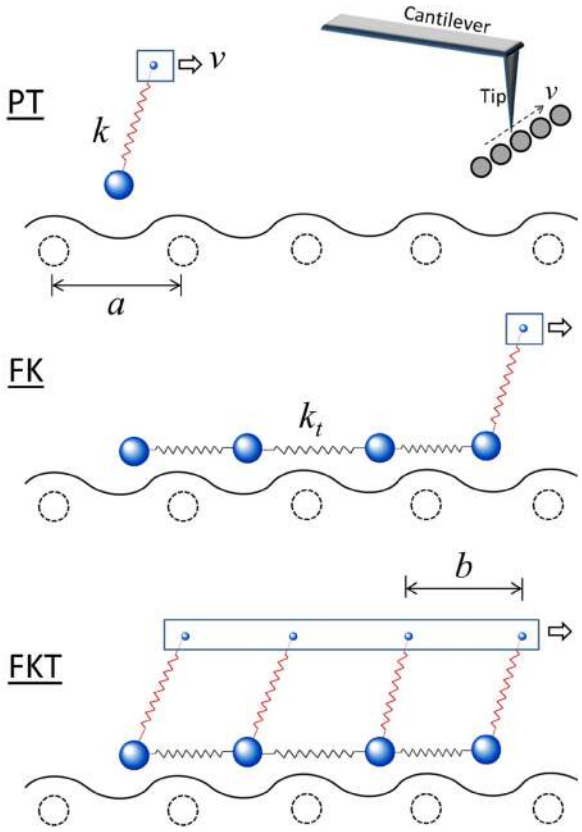

FIG. 13. Illustrations of the 1-D PT, FK, and FKT models. Large solid spheres represent tip atoms and rectangular slabs represent the sliding support. Inset is a schematic highlighting the relationship between an AFM tip/cantilever and the simple mass-spring model. Reprinted with permission from Dong *et al.*, Tribol. Lett. **44**, 367 (2011). Copyright 2011 Springer Nature.

decade.[146–149] This approach was finally implemented in 2015 with laser-cooled $^{174}Yb^{+}$ ions held in a linear Paul trap moving over the sinusoidal potential of an optical standing wave.[21] A schematic of the experiment is shown in Fig. 14. With this approach, the relative mismatch of the ion spacing and the spacing of the optical lattice can be freely varied as well as the speed of the Paul trap with respect to the optical lattice.

This experimental approach opened up a unique way to explore superlubricity and showed behavior consistent with the simple 1-D FK/FKT models. For example, it was found

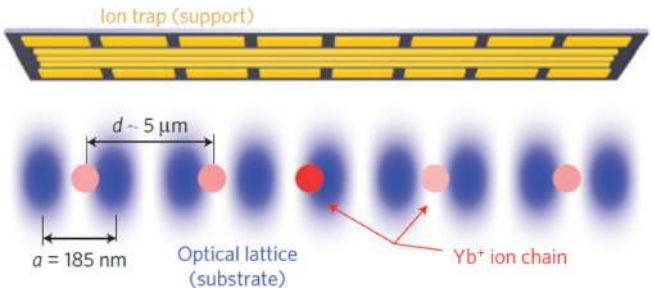

FIG. 14. Illustration of the experimental implementation of a cold trapped ion chain and a sinusoidal optical lattice. The lattice spacing of the chain relative to the optical standing wave can be varied to yield differing levels of commensurability. Reprinted with permission from Bylinskii *et al.*, Nat. Mater. **15**, 717 (2016). Copyright 2016 Springer Nature.

that superlubricity could be achieved when the two lattice spacings were optimally mismatched and that both thermolubricity and structural superlubricity contributed to the observed ultra-low friction.[21] This topic was further explored with a two-ion system tested at velocities ranging over five orders of magnitude. The results showed that structural superlubricity enables ultra-low friction when the potential barrier is much greater than k_BT, but that thermal lubricity dominates when the potential barrier is similar to k_BT.[150] Based on that study, the authors identified and explored a regime where friction was minimally affected by temperature, so pure structural superlubricity could be observed. These measurements were used to reproduce the theoretically predicted Aubry transition; above the transition, the chain is flexible enough for the atoms to conform (be pinned) to the underlying potential leading to stick-slip; below the transition, the chain is too rigid for this to occur, leading to smooth sliding and superlubricity.[73] Such studies were also extended beyond single slip to reproduce trends in friction from multiple slips.[151] Finally, incommensurability was introduced via defects (as opposed to relative lattice spacing) in a study that showed a transition from sticking to continuous sliding, with behavior similar to that expected from an Aubry transition.[152]

Many of the papers cited in the previous paragraph conclude by suggesting that this approach may be used to demonstrate *quantum lubricity*.[73,150–152] The term quantum lubricity describes the concept that smooth sliding could occur if ions tunnel through the energy barriers, as opposed to hopping over them, as illustrated in Fig. 15. Although this idea has not yet been proven experimentally, a recent theoretical paper showed that it should be possible with the cold trapped ion experiments if the particles are cold enough.[22] If quantum lubricity is realized experimentally, this may open up entirely new avenues for friction control and the field of superlubricity.

VII. CONCLUSIONS AND PERSPECTIVES ON FUTURE RESEARCH

The main aim of this review has been to introduce the idea of superlubricity in its various manifestations, present an overview of related physical mechanisms, and summarize recent theoretical and experimental research developments. While the present work in no way represents an exhaustive list of achievements in the field, the discussed content nevertheless shows the immense progress in our fundamental understanding of this exciting topic since the first theoretical predications of superlubricity by Hirano in the early 1990s. While a complete and unifying physical picture of superlubricity relying on first principles is yet to be formed, research in the field is slowly moving toward proof-of-concept applications, with future technological implications.

Among the superlubricity mechanisms discussed, structural superlubricity is perhaps the most straightforward to understand, as it is, in its essence, a purely structural/geometrical phenomenon. Despite its basic physical principles, structural superlubricity was long thought to be only a scientific exercise because most conventional engineering

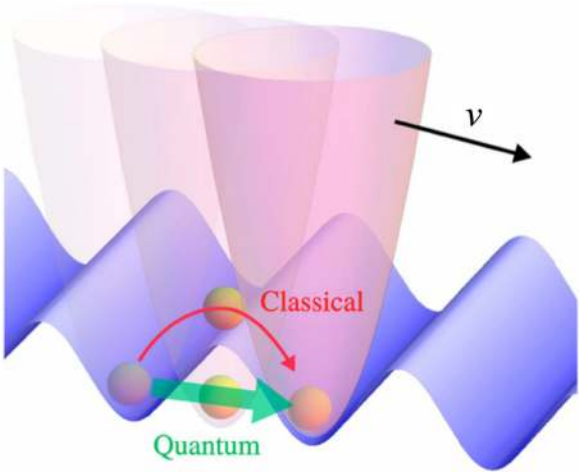

FIG. 15. Schematic illustration of the concept of quantum lubricity. A particle dragged by a confining potential (pink, imposed by the Paul trap in the experiments), moving over a periodic potential landscape (blue, corresponding to the optical lattice in the experiments) with velocity v. The green arrow shows quantum tunneling through the barrier as opposed to the classical overcoming of the barrier shown by the red arrow. Reprinted with permission from Zanca *et al*., Proc. Natl. Acad. Sci. U. S. A. **115**, 3547 (2018). Copyright 2018 National Academy of Sciences.

applications operate in ambient setting and without molecularly clean interfaces. Remarkably, experiments performed in the last few years have demonstrated that structural superlubricity may indeed be achieved under ambient conditions, for instance, in carbon-based materials such as HOPG[15] and carbon nanotubes.[53] While this discovery has already paved the way for proposals involving, e.g., graphitic micro-scale mechanical devices[153,154] devoid of friction-induced effects such as wear (a significant issue for small-scale devices due to large surface-to-volume ratios[155]), implications for technological applications significantly expanded after the demonstration of structural superlubricity between dissimilar materials (in particular, noble metals and HOPG) under ambient conditions.[16,66]

Since the presumed requirement of pristine vacuum environments has now been overcome, the main remaining challenge for applying the concept of structural superlubricity to engineering applications is increasing the size scale (in systems that do not necessarily involve the inherently smooth shearing of graphitic layers in certain carbon-based materials[15,53]). As was the case for molecularly clean environments a few years ago, the prospects look dim: With increasing contact area, elastic deformation leads to isolated regions of commensurate alignment between slider and substrate, and a resulting breakdown of superlubric behavior[69–71]—now confirmed by manipulation experiments on nano islands,[65] laser-cooled ions,[73] and colloidal monolayers.[72] However, several reasonable approaches to overcoming the elasticity-induced size limit exist. For instance, since amorphous materials typically have much higher stiffness and fundamentally different deformation mechanisms than their crystalline counterparts, the use of amorphous sliders and/or substrates is an avenue that will certainly be explored in future theoretical work and experiments.

Another approach to achieving superlubric states in technologically relevant applications (for instance, in MEMS devices) could involve the implementation of contact actuation discussed in Sec. III. The main advantage of the contact actuation technique over the method of normal force control (also discussed in Sec. III) lies in the fact that procedures for applying a periodic voltage between surfaces at or near contact readily exist for many electro-mechanical systems. For instance, electrostatic actuation has been recently used to suppress adhesion at the high speed sliding interface formed between the head and disk components of a hard disk drive.[156] On the other hand, the significant advantage of *inherent superlubricity* associated with structurally superlubric material combinations is lost in this case, as the design, fabrication, and/or integration of additional components for mechanical systems under consideration are needed for the realization of contact actuation.

Temperature has been shown to have a significant effect on friction (in the form of thermal activation at increasing temperatures, enabling the slider to overcome the potential energy barriers imposed by interactions with the substrate), which suggests that it may be possible to achieve superlubric sliding by an increase in temperature only: through *thermolubricity*, as discussed in Sec. IV. However, the observation of thermolubricity as a self-standing phenomenon isolated from other mechanisms contributing to superlubricity is experimentally very challenging. Moreover, the theoretically predicted transition to the thermal drift regime, signified by ultra-low friction forces that depend linearly on velocity, has not yet been experimentally verified. Regardless, the contribution of thermal effects to the observation of superlubricity in certain milestone experiments is clear,[11] which encourages further work in this challenging area.

Liquid superlubricity presents intriguing opportunities, as it does not suffer from many of the physical limitations associated with other superlubricity mechanisms, such as the elasticity-induced size limitation of structural superlubricity at dry, crystalline interfaces. Superlubricity can be achieved in liquid-lubricated interfaces with systems that exhibit several key features: smooth surfaces, low viscosity liquids, sufficient load support, and low shear resistance. Most research efforts have addressed the first two requirements by explicitly measuring on ultra-smooth surfaces and with very low viscosity fluids (most commonly, aqueous solutions), so the focus has recently been on identifying systems that can exhibit both appreciable load support and low shear. However, implementation of liquid superlubricity beyond the laboratory will require revising the first two requirements. First, conventional engineering components are likely to be rough; the typical average roughness of a plain bearing surface is 1 μm, compared to 5 nm or less in most liquid superlubricity studies. Second, conventional engineering components are almost always lubricated with oil, which is much more viscous than fluids used to demonstrate superlubricity; a typical engine oil viscosity is 80 mPa·s at 40 °C, compared to, e.g., 0.65 mPa·s for water. Further, lubricating oils contain additives that perform specific functions in the lubricant, such as changing the rate of viscosity decrease with temperature or keeping wear particles suspended in the oil, that are not present in superlubricity studies. Therefore, there is a significant gap between the conditions under which

liquid superlubricity has been observed and those associated with many practical applications. To overcome this gap, researchers may apply the novel ideas used to resolve the load support–low shear conflict in idealized cases to more widely relevant application conditions. Some of the superlubricity mechanisms may not be directly extensible beyond water lubrication, such as a hydration layers,[18] but others might be adapted or modified for lubricating oils, such as tribofilm formation.[119] Identifying and extending liquid superlubricity mechanisms, such that they can be observed under a wider range of conditions, is an important direction for future research in this area, with the potential to have a significant impact on engineering applications that rely on liquid lubrication.

Finally, recent experimental developments (specifically the ability to precisely control the motion of laser-cooled ions on optical standing waves) have enabled the direct validation of the simple 1-D theories used to describe structural and thermal superlubricity.[21] Such experiments have also demonstrated that it is possible to decouple the effects of these two mechanisms.[150] Also, at or near the end of many of the papers reporting these findings, researchers suggest that the same approach may be used to measure quantum lubricity, the concept that ultra-low friction sliding (i.e., superlubricity) could be achieved if ions tunnel through energy barriers as opposed to hopping over them. Theoretical analysis suggests that quantum lubricity could be measured using the laser-cooled ion approach.[22] However, at this point, it has not yet been experimentally observed. If quantum lubricity is indeed measured, entirely new directions for superlubricity research would appear, with the aim of comprehensively characterizing this exciting mechanism. Although its effect may be small in conventional friction systems, exploring how quantum lubricity could potentially be leveraged for friction control under specific conditions (such as very low temperatures) is an exciting fundamental research direction.

Considering the many different approaches to achieving superlubricity discussed in this review together, it is possible that they all fit within a single theoretical framework: A thermally activated point mass (or a collection of point masses) dragged over a potential energy surface by elastic tether(s) (i.e., spring(s)), as described by the Prandtl-Tomlinson and Frenkel-Kontorova models. In these simple models, friction (the lateral force in the tether) increases as long as the mass is stuck in a given potential energy well. Reducing friction is then possible by facilitating movement of the mass from one energy well into the next. This can be achieved by lowering the energy barrier, increasing the thermal energy of the mass, creating a lower (i.e., "softer") energy barrier, or enabling the mass to tunnel through the barrier. These four concepts are realized practically in the different approaches to superlubricity: the energy barrier can be lowered by sliding surfaces in incommensurate configurations (structural superlubricity), reducing the normal force, or actuating the contact; thermal energy is increased at higher temperatures (thermolubricity); use of a liquid interface between solid surfaces is consistent with the idea of softening the relevant energy barriers such that they can be elastically lowered; and, although only conceptual at this point, tunneling through barriers can be achieved through quantum lubricity. Thus, despite the widely varying materials and methods used in studies of superlubricity, there is an underlying goal: to reduce the effort (i.e., friction) required for relative lateral motion of surfaces at an interface. Thinking of superlubricity in this unified way may lead to new ideas regarding how to achieve it, very different from those that have already been explored. For example, while significant research has focused on decreasing energy barriers and increasing thermal activation, perhaps future studies could explore ways to physically control the properties of the elastic tether, or come up with new ways of "coupling" the tether to the energy barriers. Entirely new avenues of achieving superlubricity may be possible, built on the basic concepts and models of frictional sliding.

Overall, it is certainly an exciting time for researchers from various fields working on superlubricity, as the rate of research progress is accelerating rapidly, and the physical limitations that were once thought to confine superlubric behavior to extreme conditions (such as a pristine vacuum environment and the nanometer scale) are now being overcome. It is projected that further fundamental scientific discovery will ultimately enable notable technological advances, initially for mechanical systems on the nano- and micrometer scale, and then potentially on conventional engineering length scales. Within this context, the application of superlubricity toward mechanical systems employed in space exploration (where energy is at a premium and mechanical failure due to friction-induced issues can be critical[157]) emerges as a promising niche area. Once the promise of superlubricity is realized for such specialty cases, it is likely that the successes will lead to research focused on extending the application range of technological developments, ultimately enabling a sustainable state of ultra-low friction and transformative improvements in the efficiency of mechanical systems.

ACKNOWLEDGMENTS

M.R.V. and A.M. acknowledge support from the U.S. National Science Foundation through Grant No. CMMI-1362565.

[1]K. Holmberg and A. Erdemir, Friction **5**, 263 (2017).
[2]M. Hirano and K. Shinjo, Phys. Rev. B **41**, 11837 (1990).
[3]K. Shinjo and M. Hirano, Surf. Sci. **283**, 473 (1993).
[4]J. B. Sokoloff, Phys. Rev. B **42**, 760 (1990).
[5]M. H. Muser, Europhys. Lett. **66**, 97 (2004).
[6]J. M. Martin and A. Erdemir, Phys. Today **71**(4), 40 (2018).
[7]M. Hirano, K. Shinjo, R. Kaneko, and Y. Murata, Phys. Rev. Lett. **67**, 2642 (1991).
[8]M. Hirano and K. Shinjo, Wear **168**, 121 (1993).
[9]J. M. Martin, C. Donnet, T. Lemogne, and T. Epicier, Phys. Rev. B **48**, 10583 (1993).
[10]M. Dienwiebel, G. S. Verhoeven, N. Pradeep, J. W. M. Frenken, J. A. Heimberg, and H. W. Zandbergen, Phys. Rev. Lett. **92**, 126101 (2004).
[11]S. Y. Krylov, K. B. Jinesh, H. Valk, M. Dienwiebel, and J. W. M. Frenken, Phys. Rev. E **71**, 065101 (2005).
[12]K. B. Jinesh, S. Y. Krylov, H. Valk, M. Dienwiebel, and J. W. M. Frenken, Phys. Rev. B **78**, 155440 (2008).
[13]A. Socoliuc, R. Bennewitz, E. Gnecco, and E. Meyer, Phys. Rev. Lett. **92**, 134301 (2004).

[14]A. Socoliuc, E. Gnecco, S. Maier, O. Pfeiffer, A. Baratoff, R. Bennewitz, and E. Meyer, Science **313**, 207 (2006).
[15]Z. Liu, J. R. Yang, F. Grey, J. Z. Liu, Y. L. Liu, Y. B. Wang, Y. L. Yang, Y. Cheng, and Q. S. Zheng, Phys. Rev. Lett. **108**, 205503 (2012).
[16]E. Cihan, S. Ipek, E. Durgun, and M. Z. Baykara, Nat. Commun. **7**, 12055 (2016).
[17]D. Berman, S. A. Deshmukh, S. K. R. S. Sankaranarayanan, A. Erdemir, and A. V. Sumant, Science **348**, 1118 (2015).
[18]J. Klein, Friction **1**, 1 (2013).
[19]J. J. Li, C. H. Zhang, L. R. Ma, Y. H. Liu, and J. B. Luo, Langmuir **29**, 271 (2013).
[20]H. Li, R. J. Wood, M. W. Rutland, and R. Atkin, Chem. Commun. **50**, 4368 (2014).
[21]A. Bylinskii, D. Gangloff, and V. Vuletic, Science **348**, 1115 (2015).
[22]T. Zanca, F. Pellegrini, G. E. Santoro, and E. Tosatti, Proc. Natl. Acad. Sci. U. S. A. **115**, 3547 (2018).
[23]A. Erdemir and J. M. Martin, *Superlubricity* (Elsevier, 2007).
[24]E. Gnecco, S. Maier, and E. Meyer, J. Phys.: Condens. Matter **20**, 354004 (2008).
[25]J. J. Li and J. B. Luo, Sci. China: Technol. Sci. **56**, 2877 (2013).
[26]E. Meyer and E. Gnecco, Friction **2**, 106 (2014).
[27]Q. S. Zheng and Z. Liu, Friction **2**, 182 (2014).
[28]D. Dietzel, U. D. Schwarz, and A. Schirmeisen, Friction **2**, 114 (2014).
[29]D. Berman, A. Erdemir, and A. V. Sumant, ACS Nano **12**, 2122 (2018).
[30]M. H. Muser, L. Wenning, and M. O. Robbins, Phys. Rev. Lett. **86**, 1295 (2001).
[31]M. Dienwiebel, E. de Kuyper, L. Crama, J. W. M. Frenken, J. A. Heimberg, D. J. Spaanderman, D. G. van Loon, T. Zijlstra, and E. van der Drift, Rev. Sci. Instrum. **76**, 043704 (2005).
[32]M. Dienwiebel, N. Pradeep, G. S. Verhoeven, H. W. Zandbergen, and J. W. M. Frenken, Surf. Sci. **576**, 197 (2005).
[33]Y. Dong, Q. Li, J. Wu, and A. Martini, Modell. Simul. Mater. Sci. Eng. **19**, 065003 (2011).
[34]W. Kim and M. Falk, Phys. Rev. B **80**, 235428 (2009).
[35]M. Igarashi, A. Natori, and J. Nakamura, Phys. Rev. B **78**, 165427 (2008).
[36]M. Weiss and F. J. Elmer, Phys. Rev. B **53**, 7539 (1996).
[37]G. He, M. H. Muser, and M. O. Robbins, Science **284**, 1650 (1999).
[38]A. E. Filippov, M. Dienwiebel, J. W. M. Frenken, J. Klafter, and M. Urbakh, Phys. Rev. Lett. **100**, 046102 (2008).
[39]A. S. de Wijn, C. Fusco, and A. Fasolino, Phys. Rev. E **81**, 046105 (2010).
[40]X. F. Feng, S. Kwon, J. Y. Park, and M. Salmeron, ACS Nano **7**, 1718 (2013).
[41]M. M. van Wijk, M. Dienwiebel, J. W. M. Frenken, and A. Fasolino, Phys. Rev. B **88**, 235423 (2013).
[42]Q. S. Zheng, B. Jiang, S. P. Liu, Y. X. Weng, L. Lu, Q. K. Xue, J. Zhu, Q. Jiang, S. Wang, and L. M. Peng, Phys. Rev. Lett. **100**, 067205 (2008).
[43]Z. Ye, A. Otero-de-la-Roza, E. R. Johnson, and A. Martini, Nanotechnology **25**, 425703 (2014).
[44]J. R. Yang, Z. Liu, F. Grey, Z. P. Xu, X. D. Li, Y. L. Liu, M. Urbakh, Y. Cheng, and Q. S. Zheng, Phys. Rev. Lett. **110**, 255504 (2013).
[45]Z. Liu, P. Boggild, J. R. Yang, Y. Cheng, F. Grey, Y. L. Liu, L. Wang, and Q. S. Zheng, Nanotechnology **22**, 265706 (2011).
[46]E. Koren, E. Loertscher, C. Rawlings, A. W. Knoll, and U. Duerig, Science **348**, 679 (2015).
[47]H. Deng, M. Ma, Y. Song, Q. He, and Q. Zheng, Nanoscale **10**, 14314 (2018).
[48]C. C. Vu, S. M. Zhang, M. Urbakh, Q. Y. Li, Q. C. He, and Q. S. Zheng, Phys. Rev. B **94**, 081405(R) (2016).
[49]Z. Ye, A. Otero-de-la-Roza, E. R. Johnson, and A. Martini, Nanotechnology **26**, 165701 (2015).
[50]H. Li, J. H. Wang, S. Gao, Q. Chen, L. M. Peng, K. H. Liu, and X. L. Wei, Adv. Mater. **29**, 1701474 (2017).
[51]D. Mandelli, I. Leven, O. Hod, and M. Urbakh, Sci. Rep. **7**, 10851 (2017).
[52]Y. Song, D. Mandelli, O. Hod, M. Urbakh, M. Ma, and Q. Zheng, Nature Materials **17**, 894 (2018).
[53]R. Zhang, Z. Ning, Y. Zhang, Q. Zheng, Q. Chen, H. Xie, Q. Zhang, W. Qian, and F. Wei, Nat. Nanotechnol. **8**, 912 (2013).
[54]M. Ternes, C. P. Lutz, C. F. Hirjibehedin, F. J. Giessibl, and A. J. Heinrich, Science **319**, 1066 (2008).
[55]G. Langewisch, J. Falter, H. Fuchs, and A. Schirmeisen, Phys. Rev. Lett. **110**, 036101 (2013).
[56]S. Kawai, A. Benassi, E. Gnecco, H. Soede, R. Pawlak, X. Feng, K. Muellen, D. Passerone, C. A. Pignedoli, P. Ruffieux, R. Fasel, and E. Meyer, Science **351**, 957 (2016).
[57]L. Gigli, N. Manini, A. Benassi, E. Tosatti, A. Vanossi, and R. Guerra, 2D Mater. **4**, 045003 (2017).
[58]L. Gigli, N. Manini, E. Tosatti, R. Guerra, and A. Vanossi, Nanoscale **10**, 2073 (2018).
[59]N. Varini, A. Vanossi, R. Guerra, D. Mandelli, R. Capozza, and E. Tosatti, Nanoscale **7**, 2093 (2015).
[60]D. Dietzel, T. Monninghoff, L. Jansen, H. Fuchs, C. Ritter, U. D. Schwarz, and A. Schirmeisen, J. Appl. Phys. **102**, 084306 (2007).
[61]D. Dietzel, C. Ritter, T. Monninghoff, H. Fuchs, A. Schirmeisen, and U. D. Schwarz, Phys. Rev. Lett. **101**, 125505 (2008).
[62]D. Dietzel, T. Monninghoff, C. Herding, M. Feldmann, H. Fuchs, B. Stegemann, C. Ritter, U. D. Schwarz, and A. Schirmeisen, Phys. Rev. B **82**, 035401 (2010).
[63]D. Dietzel, M. Feldmann, U. D. Schwarz, H. Fuchs, and A. Schirmeisen, Phys. Rev. Lett. **111**, 235502 (2013).
[64]C. Ritter, M. Z. Baykara, B. Stegemann, M. Heyde, K. Rademann, J. Schroers, and U. D. Schwarz, Phys. Rev. B **88**, 045422 (2013).
[65]D. Dietzel, J. Brndiar, I. Stich, and A. Schirmeisen, ACS Nano **11**, 7642 (2017).
[66]A. Ozogul, S. Ipek, E. Durgun, and M. Z. Baykara, Appl. Phys. Lett. **111**, 211602 (2017).
[67]A. S. de Wijn, Phys. Rev. B **86**, 085429 (2012).
[68]S. Aubry, *Solitons and Condensed Matter Physics* (Springer, 1978), pp. 264–277.
[69]M. Ma, A. Benassi, A. Vanossi, and M. Urbakh, Phys. Rev. Lett. **114**, 055501 (2015).
[70]A. Benassi, M. Ma, M. Urbakh, and A. Vanossi, Sci. Rep. **5**, 16134 (2015).
[71]T. A. Sharp, L. Pastewka, and M. O. Robbins, Phys. Rev. B **93**, 121402(R) (2016).
[72]T. Brazda, A. Silva, N. Manini, A. Vanossi, R. Guerra, E. Tosatti, and C. Bechinger, Phys. Rev. X **8**, 011050 (2018).
[73]A. Bylinskii, D. Gangloff, I. Counts, and V. Vuletic, Nat. Mater. **15**, 717 (2016).
[74]D. Berman, B. Narayanan, M. J. Cherukara, S. Sankaranarayanan, A. Erdemir, A. Zinovev, and A. V. Sumant, Nat. Commun. **9**, 1164 (2018).
[75]Z. Gong, C. Bai, L. Qiang, K. Gao, J. Zhang, and B. Zhang, Diamond Relat. Mater. **87**, 172 (2018).
[76]S. W. Liu, H. P. Wang, Q. Xu, T. B. Ma, G. Yu, C. H. Zhang, D. C. Geng, Z. W. Yu, S. G. Zhang, W. Z. Wang, Y. Z. Hu, H. Wang, and J. B. Luo, Nat. Commun. **8**, 14029 (2017).
[77]J. J. Li, T. Y. Gao, and J. B. Luo, Adv. Sci. **5**, 1700616 (2018).
[78]C. M. Mate, G. M. McClelland, R. Erlandsson, and S. Chiang, Phys. Rev. Lett. **59**, 1942 (1987).
[79]S. Fujisawa, Y. Sugawara, S. Morita, S. Ito, S. Mishima, and T. Okada, J. Vac. Sci. Technol., B **12**, 1635 (1994).
[80]R. Luthi, E. Meyer, M. Bammerlin, L. Howald, H. Haefke, T. Lehmann, C. Loppacher, H. J. Guntherodt, T. Gyalog, and H. Thomas, J. Vac. Sci. Technol., B **14**, 1280 (1996).
[81]R. Bennewitz, T. Gyalog, M. Guggisberg, M. Bammerlin, E. Meyer, and H. J. Guntherodt, Phys. Rev. B **60**, R11301 (1999).
[82]J. A. Hammerschmidt, W. L. Gladfelter, and G. Haugstad, Macromolecules **32**, 3360 (1999).
[83]L. Prandtl, Z. Angew. Math. Mech. **8**, 85 (1928).
[84]G. A. Tomlinson, Philos. Mag. Ser. **7**, 905 (1929).
[85]M. Dienwiebel and J. W. M. Frenken, *Fundamentals of Friction and Wear on the Nanoscale*, 2nd ed. (Springer, 2015), pp. 139–156.
[86]E. Gnecco, R. Roth, and A. Baratoff, Phys. Rev. B **86**, 035443 (2012).
[87]W. Zhong and D. Tomanek, Phys. Rev. Lett. **64**, 3054 (1990).
[88]E. Riedo, E. Gnecco, R. Bennewitz, E. Meyer, and H. Brune, Phys. Rev. Lett. **91**, 084502 (2003).
[89]S. N. Medyanik, W. K. Liu, I. H. Sung, and R. W. Carpick, Phys. Rev. Lett. **97**, 136106 (2006).
[90]E. Gnecco, A. Socoliuc, S. Maier, J. Gessler, T. Glatzel, A. Baratoff, and E. Meyer, Nanotechnology **20**, 025501 (2009).
[91]M. A. Lantz, D. Wiesmann, and B. Gotsmann, Nat. Nanotechnol. **4**, 586 (2009).
[92]P. Pedraz, R. Wannemacher, and E. Gnecco, ACS Nano **9**, 8859 (2015).
[93]O. Y. Fajardo, E. Gnecco, and J. J. Mazo, Phys. Rev. B **89**, 075423 (2014).
[94]R. Roth, O. Y. Fajardo, J. J. Mazo, E. Meyer, and E. Gnecco, Appl. Phys. Lett. **104**, 083103 (2014).

[95]X. Zhao, M. Hamilton, W. G. Sawyer, and S. S. Perry, Tribol. Lett. **27**, 113 (2007).
[96]X. Y. Zhao, S. R. Phillpot, W. G. Sawyer, S. B. Sinnott, and S. S. Perry, Phys. Rev. Lett. **102**, 186102 (2009).
[97]L. Jansen, H. Holscher, H. Fuchs, and A. Schirmeisen, Phys. Rev. Lett. **104**, 256101 (2010).
[98]I. Barel, M. Urbakh, L. Jansen, and A. Schirmeisen, Phys. Rev. Lett. **104**, 066104 (2010).
[99]I. Barel, M. Urbakh, L. Jansen, and A. Schirmeisen, Phys. Rev. B **84**, 115417 (2011).
[100]Y. Sang, M. Dubé, and M. Grant, Phys. Rev. Lett. **87**, 174301 (2001).
[101]S. Y. Krylov and J. W. M. Frenken, J. Phys.: Condens. Matter **20**, 354003 (2008).
[102]Y. Dong, D. Perez, H. Gao, and A. Martini, J. Phys.: Condens. Matter **24**, 265001 (2012).
[103]E. Gnecco, R. Bennewitz, T. Gyalog, C. Loppacher, M. Bammerlin, E. Meyer, and H. J. Guntherodt, Phys. Rev. Lett. **84**, 1172 (2000).
[104]X.-Z. Liu, Z. Ye, Y. Dong, P. Egberts, R. W. Carpick, and A. Martini, Phys. Rev. Lett. **114**, 146102 (2015).
[105]P. Steiner, R. Roth, E. Gnecco, A. Baratoff, S. Maier, T. Glatzel, and E. Meyer, Phys. Rev. B **79**, 045414 (2009).
[106]H. Iizuka, J. Nakamura, and A. Natori, Phys. Rev. B **80**, 155449 (2009).
[107]D. Perez, Y. L. Dong, A. Martini, and A. F. Voter, Phys. Rev. B **81**, 245415 (2010).
[108]H. Tomizawa and T. E. Fischer, ASLE Trans. **30**, 41 (1987).
[109]H. Spikes and W. Tysoe, Tribol. Lett. **59**, 21 (2015).
[110]A. Khajeh, X. He, J. Yeon, S. H. Kim, and S. Martini, Langmuir **34**, 5971 (2018).
[111]J. G. Xu and K. Kato, Wear **245**, 61 (2000).
[112]M. Chen, K. Kato, and K. Adachi, Wear **250**, 246 (2001).
[113]M. Chen, K. Kato, and K. Adachi, Tribol. Lett. **11**, 23 (2001).
[114]F. Zhou, X. Wang, K. Kato, and Z. Dai, Wear **263**, 1253 (2007).
[115]J. J. Li, C. H. Zhang, and J. B. Luo, Langmuir **27**, 9413 (2011).
[116]J. J. Li, C. H. Zhang, L. Sun, X. C. Lu, and J. B. Luo, Langmuir **28**, 15816 (2012).
[117]J. J. Li, C. H. Zhang, and J. B. Luo, RSC Adv. **4**, 45735 (2014).
[118]J. Li, C. Zhang, and J. Luo, Langmuir **29**, 5239 (2013).
[119]C. Matta, L. Joly-Pottuz, M. I. D. Bouchet, and J. M. Martin, Phys. Rev. B **78**, 085436 (2008).
[120]Q. F. Zeng and G. N. Dong, Tribol. Lett. **52**, 47 (2013).
[121]Q. Zeng, G. Dong, and J. M. Martin, Sci. Rep. **6**, 29992 (2016).
[122]N. Walters and A. Martini, "Friction dependence on surface roughness for castor oil lubricated NiTi alloy sliding on steel," Tribol. Trans. (to be published).
[123]U. Raviv and J. Klein, Science **297**, 1540 (2002).
[124]L. R. Ma, A. Gaisinskaya-Kipnis, N. Kampf, and J. Klein, Nat. Commun. **6**, 6060 (2015).
[125]Y. S. Leng and P. T. Cummings, J. Chem. Phys. **124**, 074711 (2006).
[126]H. P. Xiao, Tribol. Trans. **60**, 20 (2017).
[127]S. Perkin, T. Albrecht, and J. Klein, Phys. Chem. Chem. Phys. **12**, 1243 (2010).
[128]O. Y. Fajardo, F. Bresme, A. A. Kornyshev, and M. Urbakh, Sci. Rep. **5**, 7698 (2015).
[129]H. Li, M. W. Rutland, and R. Atkin, Phys. Chem. Chem. Phys. **15**, 14616 (2013).
[130]G. Mordukhovich, J. Qu, J. Y. Howe, S. Bair, B. Yu, H. M. Luo, D. J. Smolenski, P. J. Blau, B. C. Bunting, and S. Dai, Wear **301**, 740 (2013).
[131]J. Klein, E. Kumacheva, D. Mahalu, D. Perahia, and L. J. Fetters, Nature **370**, 634 (1994).
[132]U. Raviv, S. Giasson, N. Kampf, J. F. Gohy, R. Jerome, and J. Klein, Nature **425**, 163 (2003).
[133]M. Muller, S. Lee, H. A. Spikes, and N. D. Spencer, Tribol. Lett. **15**, 395 (2003).
[134]X. P. Yan, S. S. Perry, N. D. Spencer, S. Pasche, S. M. De Paul, M. Textor, and M. S. Lim, Langmuir **20**, 423 (2004).
[135]T. Drobek and N. D. Spencer, Langmuir **24**, 1484 (2008).
[136]M. Chen, W. H. Briscoe, S. P. Armes, and J. Klein, Science **323**, 1698 (2009).
[137]A. Nomura, K. Okayasu, K. Ohno, T. Fukuda, and Y. Tsujii, Macromolecules **44**, 5013 (2011).
[138]T. Ron, I. Javakhishvili, S. Hvilsted, K. Jankova, and S. Lee, Adv. Mater. Interfaces **3**, 1500472 (2016).
[139]U. Raviv, S. Giasson, N. Kampf, J. F. Gohy, R. Jerome, and J. Klein, Langmuir **24**, 8678 (2008).
[140]A. A. Pitenis, J. M. Uruena, K. D. Schulze, R. M. Nixon, A. C. Dunn, B. A. Krick, W. G. Sawyer, and T. E. Angelini, Soft Matter **10**, 8955 (2014).
[141]J. M. Uruena, A. A. Pitenis, R. M. Nixona, K. D. Schulze, T. E. Angelini, and W. G. Sawyer, Biotribology **1–2**, 24 (2015).
[142]A. A. Pitenis, J. M. Uruena, A. C. Cooper, T. E. Angelini, and W. G. Sawyer, J. Tribol. **138**, 042103 (2016).
[143]J. Frenkel and T. Kontorova, J. Phys.-USSR **1**, 137 (1939).
[144]O. M. Braun and Y. S. Kivshar, *The Frenkel-Kontorova Model: Concepts, Methods, and Applications* (Springer, 2004).
[145]Y. Dong, A. Vadakkepatt, and A. Martini, Tribol. Lett. **44**, 367 (2011).
[146]I. Garcia-Mata, O. V. Zhirov, and D. L. Shepelyansky, Eur. Phys. J. D **41**, 325 (2007).
[147]A. Benassi, A. Vanossi, and E. Tosatti, Nat. Commun. **2**, 236 (2011).
[148]T. Pruttivarasin, M. Ramm, I. Talukdar, A. Kreuter, and H. Haffner, New J. Phys. **13**, 075012 (2011).
[149]D. Mandelli, A. Vanossi, and E. Tosatti, Phys. Rev. B **87**, 195418 (2013).
[150]D. Gangloff, A. Bylinskii, I. Counts, W. Jhe, and V. Vuletic, Nat. Phys. **11**, 915 (2015).
[151]I. Counts, D. Gangloff, A. Bylinskii, J. Hur, R. Islam, and V. Vuletic, Phys. Rev. Lett. **119**, 043601 (2017).
[152]J. Kiethe, R. Nigmatullin, D. Kalincev, T. Schmirander, and T. E. Mehlstaubler, Nat. Commun. **8**, 15364 (2017).
[153]S. Y. Kim, S. Y. Cho, K. S. Kim, and J. W. Kang, Phys. E **50**, 44 (2013).
[154]H. J. Hwang and J. W. Kang, Phys. E **56**, 17 (2014).
[155]M. Urbakh, J. Klafter, D. Gourdon, and J. Israelachvili, Nature **430**, 525 (2004).
[156]S. Rajauria, O. Ruiz, S. V. Canchi, E. Schreck, and Q. Dai, Phys. Rev. Lett. **120**, 026101 (2018).
[157]M. R. Johnson, "The Galileo high gain antenna deployment anomaly," in *Proceedings of 28th Aerospace Mechanisms Symposium* (NASA Lewis Research Center, Cleveland, 1994), pp. 359–377.